

Four-dimensional $\mathcal{N} = 2$ superconformal long circular quivers

M. Beccaria^a and G.P. Korchemsky^{b,1}

^a*Università del Salento, Dipartimento di Matematica e Fisica “Ennio De Giorgi”,
and I.N.F.N. - sezione di Lecce,
Via Arnesano, I-73100 Lecce, Italy*

^b*Institut de Physique Théorique, Université Paris Saclay, CNRS,
91191 Gif-sur-Yvette, France*

E-mail: matteo.beccaria@le.infn.it, gregory.korchemsky@ipht.fr

ABSTRACT: We study four-dimensional $\mathcal{N} = 2$ superconformal circular, cyclic symmetric quiver theories which are planar equivalent to $\mathcal{N} = 4$ super Yang-Mills. We use localization to compute nonplanar corrections to the free energy and the circular half-BPS Wilson loop in these theories for an arbitrary number of nodes, and examine their behaviour in the limit of long quivers. Exploiting the relationship between the localization quiver matrix integrals and an integrable Bessel operator, we find a closed-form expression for the leading nonplanar correction to both observables in the limit when the number of nodes and 't Hooft coupling become large. We demonstrate that it has different asymptotic behaviour depending on how the two parameters are compared, and interpret this behaviour in terms of properties of a lattice model defined on the quiver diagram.

KEYWORDS: AdS-CFT Correspondence, Extended Supersymmetry, Matrix Models, Scale and Conformal Symmetries

ARXIV EPRINT: [2312.03836](https://arxiv.org/abs/2312.03836)

¹Unité Mixte de Recherche 3681 du CNRS.

Contents

1	Introduction and summary	1
2	Matrix model representation	6
3	Large N expansion of the free energy	12
3.1	Leading nonplanar correction	12
3.2	Next-to-leading nonplanar correction	13
3.3	Nonplanar corrections at weak and strong coupling	15
4	Free energy in the long quiver limit	18
5	Circular Wilson loop	21
A	Strong coupling expansion	24
B	Resummation	28

1 Introduction and summary

In this paper, we continue the study initiated in [1] of a special class of four-dimensional $\mathcal{N} = 2$ superconformal gauge theories which are planar equivalent to $\mathcal{N} = 4$ SYM theory. A distinguished feature of these theories is that various observables, e.g. free energy on four-sphere and circular half-BPS Wilson loop, can be computed exactly, for arbitrary value of the coupling constant and rank of the gauge group, in terms of matrix model integrals using the localization technique [2, 3]. The actual evaluation of these matrix integrals turns out to be a nontrivial task due to a complicated non-polynomial form of interaction potential. The latter is given by an infinite sum of single and double trace terms [4–7].

In the previous work [1], we developed a technique for the systematic expansion of such matrix integrals at large N and applied it to determine the nonplanar corrections in various $\mathcal{N} = 2$ superconformal theories including the two-nodes quiver theory with the gauge group $SU(N) \times SU(N)$. Here we shall apply this technique to compute the free energy and circular half-BPS Wilson loop in $\mathcal{N} = 2$ superconformal circular quiver theory for an arbitrary number of nodes $L \geq 2$. In what follows we refer to this theory as Q_L model.

The field content of the Q_L model can be represented as a circular quiver diagram shown in figure 1. This model has the $SU(N)^L$ gauge symmetry and depends in general on L independent 't Hooft couplings, one per each $SU(N)$ factor. At strong coupling, it is dual to type IIB string theory on the $AdS_5 \times (S^5/\mathbb{Z}_L)$ background [8]. The planar limit of the Q_L model was studied both at weak and strong 't Hooft couplings in [4, 7, 9–19]. For simplicity, we will assume that all couplings are equal and denote them as λ . In this case, the Q_L model coincides with the \mathbb{Z}_L orbifold of $\mathcal{N} = 4$ SYM with the $SU(LN)$ gauge group [20].

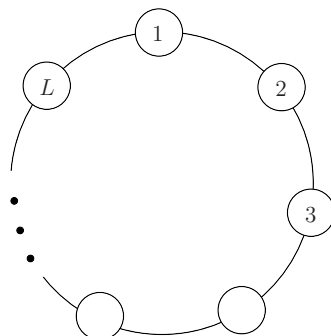


Figure 1. Diagrammatic representation of the circular quiver theory. Each node represents $SU(N)$ vector multiplet and lines connecting neighbouring nodes represent hypermultiplets in the bi-fundamental representation of $SU(N) \times SU(N)$. In the localization matrix model representation, the same diagram defines a lattice model with L sites equipped with a nearest neighbour interaction.

In the planar limit, the Q_L model is equivalent to L copies of $\mathcal{N} = 4$ SYM with the $SU(N)$ gauge group but the two models are different beyond this limit. In particular, the free energy of this model defined on the unit four-sphere has the following form

$$F_{Q_L} = LF_{\mathcal{N}=4} + \Delta F_{Q_L}, \tag{1.1}$$

where $F_{\mathcal{N}=4} = -\frac{1}{2}(N^2 - 1) \log \lambda$ is the free energy of $\mathcal{N} = 4$ SYM theory with the $SU(N)$ gauge group. The nonplanar correction to the free energy ΔF_{Q_L} admits an expansion in powers of $1/N^2$

$$\Delta F_{Q_L} = F_L^{(0)} + \frac{1}{N^2} F_L^{(1)} + O(1/N^4). \tag{1.2}$$

Our goal in this paper is to determine the dependence of the coefficient functions $F_L^{(0)}, F_L^{(1)}, \dots$ on 't Hooft coupling λ and the number of nodes L . For the simplest, two-nodes quiver $Q_{L=2}$ model, this problem was studied in [1].

Another motivation of the present work is to explore the limit of large number of nodes in the Q_L model. This limit has been previously discussed in application to superconformal theories with eight supercharges that correspond to conformal fixed points of linear quiver gauge theories in d dimensions [21–25]. In the special case of $d = 4$ relevant to our discussion, four-dimensional $\mathcal{N} = 2$ superconformal long linear quiver theories were recently analyzed at large N in [26]. Unlike the Q_L model, these theories differ from $\mathcal{N} = 4$ SYM already in the planar limit. The leading $O(N^2)$ contribution to the free energy in these theories is a nontrivial function of the number of nodes L and 't Hooft coupling. At strong coupling and large L , its asymptotic behaviour depends on the order of limits — the free energy of the long linear quiver grows as $O(N^2L)$ if the number of nodes is much larger than the 't Hooft coupling and $O(N^2L \log L)$ otherwise. In contrast, the free energy of the circular quiver theory (1.1) grows as $F_{Q_L} = O(N^2L)$ at large L , independently on the value of the 't Hooft coupling constant. We compute below the leading nonplanar correction to the free energy (1.1) and show that, similar to the planar contribution to the free energy of the long linear quiver, its asymptotic behaviour at strong coupling and large L depends on how these two parameters are compared (see eqs. (1.6) and (1.7) below).

The localization yields the partition function of the Q_L -model on the unit sphere, $Z_{Q_L} = e^{-F_{Q_L}}$, as an integral over the $SU(N)$ matrices A_I describing zero modes of scalar fields in vector multiplets at all nodes $I = 1, \dots, L$ (see (2.8) below) [2, 3]. Discussing its dependence on the number of nodes, it is advantageous to think about the quiver diagram shown in figure 1 as defining a one-dimensional lattice model with L sites. The degrees of freedom at each site are described by the matrices A_I subject to periodic boundary condition $A_{I+L} = A_I$. They interact among themselves as well as with their nearest neighbours at the sites $I \pm 1$. The form of the interaction potential is fixed by the potential of the localization matrix model. The free energy of the Q_L -model (1.1) coincides with the free energy of this lattice model.

Using this identification, the free energy F_{Q_L} can be expressed as the sum over excitations propagating across the one-dimensional lattice shown in figure 1 and interacting with each other. The number of sites can be arbitrary $2 \leq L < \infty$, but the limit of large L is of a special interest. In this limit, the lattice degenerates into a circle with circumference $O(L)$ and the free energy of the lattice model is expected to exhibit an extensive behaviour, $F_{Q_L} = O(L)$, provided that the effective interaction between different sites is short-range. The last condition depends on the values of $1/N$ and λ .

As mentioned above, the planar contribution to the free energy (1.1) grows linearly with L for an arbitrary coupling constant λ . The question arises whether the same property holds for the nonplanar correction to the free energy (1.1)

$$\Delta F_{Q_L} \stackrel{?}{=} L \varepsilon(\lambda, 1/N) + O(L^0). \tag{1.3}$$

Here the energy density $\varepsilon(\lambda, 1/N)$ depends on 't Hooft coupling and has large N expansion similar to (1.2). We show below that the relation (1.3) holds at weak coupling. At strong coupling, the validity of (1.3) depends on how L compares to $\sqrt{\lambda}$. We find that the relation (1.3) is verified for $L \gg \sqrt{\lambda} \gg 1$. In the opposite limit, for $\sqrt{\lambda} \gg L \gg 1$, the free energy ΔF_{Q_L} receives corrections that run in powers of $L/\sqrt{\lambda}$ and, therefore, violate (1.3). In this case, the lattice model becomes strongly correlated and the above mentioned condition is not satisfied.

To verify the relation (1.3), we computed the first two terms of the large N expansion of the free energy (1.2) for arbitrary number of nodes L . We show below that, for arbitrary coupling λ , they can be expressed in terms of a semi-infinite matrix whose entries are the coefficients of the double trace terms entering the potential of the localization matrix model. The same entries can be identified as matrix elements of a certain integral operator known in the mathematical literature as a truncated Bessel operator.¹ Applying the technique of [1] and exploiting the known properties of the Bessel operator, we computed $F_L^{(0)}$ and $F_L^{(1)}$ for arbitrary number of nodes L both at weak and strong coupling.

At weak coupling, the free energy ΔF_{Q_L} is given by series in 't Hooft coupling that starts at order $O(\lambda^2)$. The expansion coefficients are given by multilinear combinations of odd Riemann zeta values $\zeta(2n + 1)$ accompanied by rational L -dependent coefficients (see (3.19) and (3.20) below). Going to the limit of large L , we find that, in agreement with (1.3), the

¹It is interesting to notice that the same operator previously appeared in the study of level spacing distribution in the matrix models [27] and, more recently, in the context of the AdS/CFT correspondence [28, 29].

free energy $\Delta F_{\mathcal{Q}_L}$ grows linearly with the number of nodes

$$\Delta F_{\mathcal{Q}_L} = L \left[\frac{3\zeta(3)}{128\pi^4} \lambda^2 - \frac{15\zeta(5)}{1024\pi^6} \lambda^3 + O(\lambda^4) + O(1/N^2) \right]. \quad (1.4)$$

This behaviour is not surprising because the effective interaction between different sites of the quiver diagram in figure 1 is short range at weak coupling and, as a consequence, the free energy has an extensive behaviour.

At strong coupling, the first two terms of the expansion of the free energy (1.2) are given by

$$\begin{aligned} F_L^{(0)} &= \sqrt{\lambda} \frac{(L^2 - 1)}{6L} - \frac{1}{2}(L - 1) \log \lambda + O(\lambda^0), \\ F_L^{(1)} &= -\lambda^{3/2} \frac{(L^2 - 1)(L^2 + 1)}{1920L^3} + \lambda \frac{(L^2 - 1)(L^2 - 9)}{5760L^3} + O(\sqrt{\lambda}). \end{aligned} \quad (1.5)$$

The subleading corrections to both relations run in powers of $1/\sqrt{\lambda}$, their explicit expressions can be found in (3.30) and (3.31) below. As expected, the functions (1.5) have a nontrivial dependence on the number of nodes $2 \leq L < \infty$. For $L = 2$, the relations (1.5) reproduce the analogous expressions for the free energy in the \mathcal{Q}_2 model obtained in [1]. Notice that the functions (1.5) vanish for an unphysical value $L = 1$. In this case, the quiver diagram in figure 1 contains only one node. The corresponding localization matrix integral for $F_{\mathcal{Q}_L}$ becomes Gaussian and it coincides with the free energy of $\mathcal{N} = 4$ SYM. As a consequence, for $L = 1$ the nonplanar correction $\Delta F_{\mathcal{Q}_L}$ has to vanish for arbitrary coupling constant.

At strong coupling, we can use (1.5) to verify that for $L \gg 1$ the first few terms of the strong coupling expansion of the free energy (1.2) grow linearly with L . However the situation becomes more complicated when we include the subleading corrections in $1/\sqrt{\lambda}$. They take the following form at large L

$$\Delta F_{\mathcal{Q}_L} = L \left[\frac{1}{6} \sqrt{\lambda} - \log \frac{\sqrt{\lambda}}{4\pi} + \left(\frac{1}{4} - 6 \log \mathbf{A} \right) - \frac{1}{4\sqrt{\lambda}} \log L \right] + f\left(\frac{L}{\sqrt{\lambda}}\right) + \dots, \quad (1.6)$$

where \mathbf{A} is the Glaisher constant and dots denote corrections suppressed by powers of $1/N^2$ and $1/L$. At large L and $\sqrt{\lambda}$, the subleading corrections to (1.6) run in powers of $L/\sqrt{\lambda}$. They are described by the function $f(L/\sqrt{\lambda})$.

Remarkably, this function can be found in a closed form (see (4.6) below). It is interesting to examine its behaviour for different values of the ratio $l = L/\sqrt{\lambda}$. At small l , or equivalently $L \ll \sqrt{\lambda}$, the function $f(l)$ is given by a series in l that starts at order $O(l^2)$. The resulting expression for the free energy (1.6) contains $(L \log L)/\sqrt{\lambda}$ term and does not satisfy (1.3). The reason why the free energy (1.6) does not grow linearly with L is that the quiver lattice model becomes strongly correlated for $\sqrt{\lambda} \gg L \gg 1$, thus invalidating the relation (1.3).

At large l , or equivalently $L \gg \sqrt{\lambda}$, the function $f(l)$ behaves as $f(l) = l(\log(4\pi l) - c)/4 + O(l^0)$, where c is a constant defined in (4.7) below. Substituting this relation into (1.6) we find that the term proportional to $(L \log L)/\sqrt{\lambda}$ cancels and we recover the expected scaling behaviour (1.3)

$$\Delta F_{\mathcal{Q}_L} = L \left[\frac{1}{6} \sqrt{\lambda} - \log \frac{\sqrt{\lambda}}{4\pi} + \left(\frac{1}{4} - 6 \log \mathbf{A} \right) - \frac{1}{4\sqrt{\lambda}} \left(\log \frac{\sqrt{\lambda}}{4\pi} + c \right) \right] + O(1/N^2) + O(L^0). \quad (1.7)$$

We would like to emphasize that this relation holds for $L \gg \sqrt{\lambda} \gg 1$. As compared with (1.6), the term proportional to $\log L$ gets replaced in (1.7) with $\log(\sqrt{\lambda}/(4\pi)) + c$.

Another interesting quantity that can be computed in the Q_L model using the localization technique is the expectation value of the half-BPS circular Wilson loop defined at one of the nodes of the quiver. In virtue of planar equivalence of the Q_L model and $\mathcal{N} = 4$ SYM, the expectation value of the Wilson loops in these two theories coincide up to nonplanar corrections. We find that the leading nonplanar correction to their ratio it is proportional to a derivative of the free energy

$$\frac{W_{Q_L}}{W_{\mathcal{N}=4}} = 1 - \frac{1}{4LN^2} \lambda^2 \partial_\lambda \Delta F_{Q_L} + O(1/N^4). \tag{1.8}$$

This relation is valid for arbitrary coupling λ and the number of nodes L . Similar relation has been previously derived for other superconformal $\mathcal{N} = 2$ theories including the Q_2 model [1, 30].

At large L , the scaling behaviour (1.3) of the free energy implies that the nonplanar $O(1/N^2)$ correction to (1.8) is independent of the number of nodes L . As explained above, this property holds both at weak coupling and at strong coupling for $1 \ll \sqrt{\lambda} \ll L$. In the latter case, we have

$$\frac{W_{Q_L}}{W_{\mathcal{N}=4}} = 1 - \frac{1}{N^2} \left[\frac{\lambda^{3/2}}{48} - \frac{\lambda}{8} + \frac{\sqrt{\lambda}}{32} \left(\log \frac{\sqrt{\lambda}}{4\pi} + c - 1 \right) + O(\lambda^0) \right] + O(1/N^4) + O(1/L). \tag{1.9}$$

At very strong coupling, for $1 \ll L \ll \sqrt{\lambda}$, we find instead

$$\frac{W_{Q_L}}{W_{\mathcal{N}=4}} = 1 - \frac{1}{N^2} \left[\frac{\lambda^{3/2}}{48} - \frac{\lambda}{8} + \frac{\sqrt{\lambda}}{32} \log L + O(\lambda^0) \right] + O(1/N^4) + O(1/L). \tag{1.10}$$

Similar to the free energy, $\log L$ term inside the brackets is replaced with $\log(\sqrt{\lambda}/(4\pi)) + c - 1$ for $\sqrt{\lambda} \ll L$.

It is interesting to note that the order of limit phenomenon that we described above for the free energy and the circular Wilson loop in the long quiver limit is not a specific feature of $\mathcal{N} = 2$ superconformal theories. Analogous phenomenon has been previously observed in the study of four-point correlation functions of infinitely heavy half-BPS operators in planar $\mathcal{N} = 4$ SYM in the so-called null limit when the four operators are light-like separated in a sequential manner, $(x_i - x_{i+1})^2 \sim e^{-y}$ for $y \rightarrow \infty$ [31]. It turns out that, at strong coupling, these functions have different asymptotic behaviour for $1 \ll y \ll \sqrt{\lambda}$ and $1 \ll \sqrt{\lambda} \ll y$ [28, 32, 33].

The limit of large L can be viewed as a continuum limit of the lattice model defined on the quiver diagram shown in figure 1. The fact that the L -dependence of the free energy (1.6) is encoded in a function of the ratio $L/\sqrt{\lambda}$ suggests that interaction between excitations is characterized in this limit by a correlation length $\xi = O(\sqrt{\lambda})$. In application to the long circular quiver, we therefore expect that the correlation function of local (chiral primary) operators $O_{n,I}(x) = \text{tr}(\varphi_I^n(x))$ placed at different nodes of the quiver $|I - J| = O(L)$ has to scale as $\langle O_{n,I}(x) \bar{O}_{n,J}(0) \rangle \sim e^{-|I-J|/\xi}$.

It would be interesting to reproduce the strong coupling expansion of the free energy of the long circular quiver theory (1.6) using the AdS/CFT correspondence. In the holographic

description, the Q_L theory is dual to type IIB superstrings propagating on the orbifold $AdS_5 \times (S^5/\mathbb{Z}_L)$. To obtain the free energy, one has to determine higher-derivative string corrections to the type IIB 10d effective action. For the simplest, length $L = 2$ quiver, this problem was discussed in [1]. The remarkable simplicity of the obtained expression (1.6) (see also (4.6)) suggests that the problem can be solved in the limit of long quivers. Another interesting question is to clarify the origin of the ratio $L/\sqrt{\lambda}$ on the string side.

The rest of the paper is organized as follows. In section 2 we present the matrix model representation of the partition function of the Q_L model on the unit four-sphere. We then use it to derive a Feynman diagram representation of the first few terms in the large N expansion of the free energy (1.2). The contribution of these diagrams to the free energy is evaluated in section 3. We show that it can be expressed in a concise way in terms of matrix elements of the resolvent of the so-called Bessel kernel. We exploit this relation to derive the free energy F_{Q_L} at weak and strong coupling. In section 4 we examine behaviour of the free energy of the Q_L model in the limit of large number of nodes L . The expectation value of half-BPS circular Wilson loop is computed in section 5. Some technical details are presented in two appendices.

2 Matrix model representation

Using the localization the partition function of the quiver Q_L model defined on the unit sphere S^4 (with equal coupling constants on all nodes) can be expressed as a matrix integral [2, 3]

$$Z_{Q_L} = \int \prod_{I=1}^L \left[\prod_{r=1}^N da_{I,r} \delta\left(\sum_r a_{I,r}\right) \Delta^2(\mathbf{a}_I) \right] e^{-S_{Q_L}(\mathbf{a}_1, \dots, \mathbf{a}_L)}, \quad (2.1)$$

where integration goes over eigenvalues $\mathbf{a}_I = \{a_{I,1}, \dots, a_{I,N}\}$ of hermitian traceless $N \times N$ matrices A_I describing zero modes of a scalar field in the vector multiplet on S^4 at nodes $I = 1, \dots, L$. Here $\Delta(\mathbf{a}_I) = \prod_{r < s} (a_{I,r} - a_{I,s})$ is a Vandermonde determinant depending on the eigenvalues at the node I .

The potential in (2.1) is given by the sum of one-loop perturbative and instanton contributions. The latter can be neglected at large N leading to

$$S_{Q_L} = \sum_{I=1}^L \left[\frac{8\pi^2 N}{\lambda} \sum_{r=1}^N a_{I,r}^2 + \sum_{r,s=1}^N \left(\log H(a_{I,r} - a_{I+1,s}) - \log H(a_{I,r} - a_{I,s}) \right) \right], \quad (2.2)$$

where the periodicity condition $a_{I+L,r} = a_{I,r}$ is implied. This relation involves the H -function given by the product of the Barnes G -functions

$$\begin{aligned} H(x) &= e^{-(1+\gamma_E)x^2} G(1+ix)G(1-ix) \\ &= \exp\left(\sum_{n=1}^{\infty} \frac{(-1)^n}{n+1} \zeta(2n+1) x^{2n+2}\right), \end{aligned} \quad (2.3)$$

where the second relation holds at small x and it involves odd Riemann zeta values.

It is convenient to express the potential (2.2) in terms of traces of the hermitian matrices

$$\mathcal{O}_i(A_I) = \text{tr} \left(\frac{A_I}{\sqrt{N}} \right)^i = \sum_{r=1}^N \left(\frac{a_{I,r}}{\sqrt{N}} \right)^i, \quad (2.4)$$

where $i \geq 2$. Expanding the H -functions in (2.2) in powers of eigenvalues a_r and rescaling them as $a_r \rightarrow (8\pi^2 N/\lambda)^{-1/2} a_r$, we get

$$S_{\text{QL}} = \sum_{I=1}^L \left[\text{tr} A_I^2 - S_{\text{int}}(A_I, A_{I+1}) \right], \quad (2.5)$$

where $A_{L+1} \equiv A_1$ and the interaction term is given by infinite bilinear combinations of the single traces (2.4)

$$S_{\text{int}}(A_I, A_{I+1}) = \frac{1}{8} \sum_{i,j \geq 2} C_{ij}(\lambda) [\mathcal{O}_i(A_I) - \mathcal{O}_i(A_{I+1})] [\mathcal{O}_j(A_I) - \mathcal{O}_j(A_{I+1})]. \quad (2.6)$$

The sum does not involve $\mathcal{O}_1(A_I) = \text{tr}(A_I/\sqrt{N})$ because it vanishes for the $\text{SU}(N)$ matrices A_I . The expansion coefficients in (2.6) are different from zero only if the indices i and j have the same parity. Nonzero coefficients $C_{ij}^+(\lambda) \equiv C_{2i,2j}$ and $C_{ij}^-(\lambda) \equiv C_{2i+1,2j+1}$ are given by [14, 18]

$$\begin{aligned} C_{ij}^-(\lambda) &= 8 \left(\frac{\lambda}{8\pi^2} \right)^{i+j+1} (-1)^{i-j+1} \zeta(2(i+j) + 1) \frac{\Gamma(2(i+j) + 2)}{\Gamma(2i+2)\Gamma(2j+2)}, \\ C_{ij}^+(\lambda) &= 8 \left(\frac{\lambda}{8\pi^2} \right)^{i+j} (-1)^{i-j+1} \zeta(2(i+j) - 1) \frac{\Gamma(2(i+j))}{\Gamma(2i+1)\Gamma(2j+1)}, \end{aligned} \quad (2.7)$$

where $i, j \geq 1$. They define two semi-infinite matrices whose properties play an important role in what follows.

As mentioned in the Introduction, it proves convenient to interpret the matrix integral (2.1) as a partition function of a lattice model defined on the quiver diagram shown in figure 1²

$$Z_{\text{QL}} = \int \prod_{I=1}^L DA_I \exp \left(- \sum_{I=1}^L \left[\text{tr} A_I^2 - S_{\text{int}}(A_I, A_{I+1}) \right] \right), \quad (2.8)$$

where integration goes over $\text{SU}(N)$ matrices satisfying periodic boundary conditions $A_{I+L} = A_I$. The $\text{SU}(N)$ matrices A_I (with $I = 1, \dots, L$) describe $(N^2 - 1)$ degrees of freedom living at L sites of the lattice. The second term inside the brackets in the exponent of (2.8) defines the interaction (2.6) between the nearest neighbours on the lattice.

Topological expansion. Viewed as a matrix integral, the partition function (2.8) can be expanded at large N into a sum of two-dimensional surfaces of different genus.

A somewhat unusual property of the interaction potential (2.6) is that it is given by an infinite sum of double trace terms. Such terms are known to produce touching surfaces [34–37]. More precisely, the double-trace term of the form $C_{ij} \mathcal{O}_i(A_I) \mathcal{O}_j(A_J)$ generates the touching of two surfaces labelled by I and J . According to (2.8), the label J can take three different values $I - 1, I$ and $I + 1$, so that the surface with the label $I = 1, \dots, L$ can touch surfaces either of the same type and/or of two adjacent labels (subject to the periodicity condition).

²Going from (2.1), we changed the integration variables as $A_I \rightarrow (8\pi^2 N/\lambda)^{-1/2} A_I$. The Jacobian of this transformation coincides with the partition function of L copies of $\mathcal{N} = 4$ SYM. It is not displayed in (2.8). This is the reason why (2.8) gives the difference free energy $Z_{\text{QL}} = \exp(-\Delta F_{\text{QL}})$.

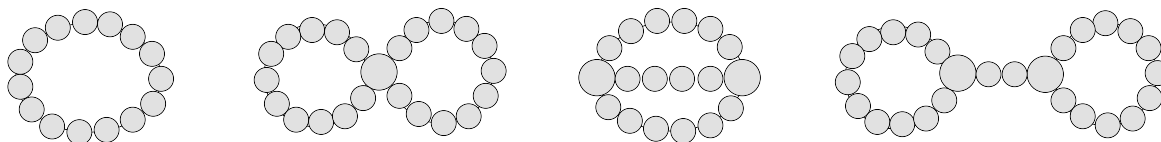


Figure 2. Surfaces arising from the topological expansion of the partition function (2.8) at large N . They are obtained by gluing together grey spheres, each carrying the label $I = 1, \dots, L$. The sphere with the label I can touch spheres with the same label and/or with label $I \pm 1$.

As a result, the surfaces arising from large N expansion of the partition function (2.8) take the form of necklaces connected with each other as shown in figure 2. The configuration with h holes provides the contribution of order $O(1/N^{2(h-1)})$. For instance, the leftmost diagram in figure 2 scales as $O(N^0)$, three remaining diagrams scale as $O(1/N^2)$. Notice that figure 2 does not contain planar diagrams with $h = 0$ (see footnote 2).

In the rest of this section, we develop a technique for computing the contribution of the diagrams shown in figure 2 to the partition function (2.8).

Hubbard-stratonovich transformation. Taking an advantage of the symmetry of the partition function (2.8) under the cyclic shift of matrices, $A_I \rightarrow A_{I+1}$, we can simplify the interaction term (2.6) by Fourier expanding the single-traces $\mathcal{O}_i(A_I)$ over modes with a definite quasimomentum $p_\alpha = 2\pi\alpha/L$

$$\mathcal{O}_i(A_I) = \frac{1}{\sqrt{L}} \sum_{\alpha=0}^{L-1} e^{ip_\alpha I} \tilde{\mathcal{O}}_{\alpha,i}, \quad (2.9)$$

where $(\tilde{\mathcal{O}}_{\alpha,i})^\dagger = \tilde{\mathcal{O}}_{-\alpha,i}$ and $i \geq 2$. As we will see in a moment, p_α has the meaning of momenta of excitations propagating across the lattice shown in figure 1. Inverse relation looks as

$$\tilde{\mathcal{O}}_{\alpha,i} = \frac{1}{\sqrt{L}} \sum_{I=1}^L e^{-ip_\alpha I} \mathcal{O}_i(A_I). \quad (2.10)$$

Substituting (2.9) into (2.6) one gets [14, 18]

$$\sum_{I=1}^L S_{\text{int}}(A_I, A_{I+1}) = \frac{1}{2} \sum_{\alpha=0}^{L-1} s_\alpha C_{ij} \tilde{\mathcal{O}}_{\alpha,i} \tilde{\mathcal{O}}_{-\alpha,j}, \quad (2.11)$$

where summation over repeated indices $i, j \geq 2$ is tacitly assumed and the notation was introduced for

$$s_\alpha = \sin^2 \left(\frac{p_\alpha}{2} \right) = \sin^2 \left(\frac{\pi\alpha}{L} \right). \quad (2.12)$$

Notice that s_α vanishes for $\alpha = 0$. As a consequence, the corresponding Fourier mode with zero quasimomentum $\tilde{\mathcal{O}}_{0,i} \sim \sum_{I=1}^L \mathcal{O}_i(A_I)$ does not contribute to (2.11) and, therefore, it is not affected by the interaction.

Following [1], we can simplify the matrix integration in (2.8) by linearizing the double-trace interaction term in (2.11). This is achieved by introducing auxiliary fields $\tilde{J}_i(p_\alpha)$

coupled to $\tilde{\mathcal{O}}_{-\alpha,i}$

$$e^{\sum_{I=1}^L S_{\text{int}}(A_I, A_{I+1})} = \mathcal{N} \int D\tilde{J} \exp \left(\sum_{\alpha=1}^{L-1} \left[\tilde{J}_i(p_\alpha) \tilde{\mathcal{O}}_{-\alpha,i} - \frac{1}{2s_\alpha} C_{ij}^{-1} \tilde{J}_i(p_\alpha) \tilde{J}_j(-p_\alpha) \right] \right). \quad (2.13)$$

Here the integration measure is $D\tilde{J} = \prod_{i,\alpha} d\tilde{J}_i(p_\alpha) d\tilde{J}_i(-p_\alpha) / (2\pi)$ and the normalization factor is given by $\mathcal{N} = (\det C)^{-(L-1)/2} (s_1 \dots s_{L-1})^{-1/2}$.

Substituting (2.13) into (2.8) we find that the integral over the matrices A_I factorizes into a product of L independent integrals

$$\int \prod_{I=1}^L DA_I \exp \left(- \sum_{I=1}^L \text{tr} A_I^2 + \sum_{\alpha=1}^{L-1} \tilde{J}_i(p_\alpha) \tilde{\mathcal{O}}_{-\alpha,i} \right) = Z(J_1) \dots Z(J_L), \quad (2.14)$$

where $Z(J_I)$ is a partition function of a Gaussian $SU(N)$ matrix model

$$\begin{aligned} Z(J_I) &= \int DA \exp \left(- \text{tr} A^2 + J_{I,i} \mathcal{O}_i(A) \right) \\ &= \exp \left(N J_{I,i} G_i + \frac{1}{2!} J_{I,i_1} J_{I,i_2} G_{i_1 i_2} + \frac{1}{3! N} J_{I,i_1} J_{I,i_2} J_{I,i_3} G_{i_1 i_2 i_3} + \dots \right), \end{aligned} \quad (2.15)$$

and the sources $J_{i,I}$ (with $i \geq 2$) are given by Fourier series analogous to (2.9)

$$J_{I,i} = \frac{1}{\sqrt{L}} \sum_{\alpha=1}^{L-1} e^{ip_\alpha I} \tilde{J}_i(p_\alpha). \quad (2.16)$$

Notice that the sum in this relation does not contain the term with $\alpha = 0$ and, as a consequence, the sources satisfy the relation $\sum_{I=1}^L J_{i,I} = 0$.

The exponent in (2.15) is given by a linear combination of (connected part of) correlation functions in a Gaussian matrix model

$$G_{i_1 \dots i_n} = N^{n-2} \langle \mathcal{O}_{i_1}(A) \dots \mathcal{O}_{i_n}(A) \rangle_{0,c} = G_{i_1 \dots i_n}^{(0)} + \frac{1}{N^2} G_{i_1 \dots i_n}^{(1)} + \dots, \quad (2.17)$$

where the subscript ‘0’ in the first relation indicates that the expectation value is evaluated with a Gaussian measure. Here the factor of N^{n-2} was inserted for convenience, it ensures that $G_{i_1 \dots i_n}$ stays finite for $N \rightarrow \infty$. The second relation in (2.17) yields the expansion of the correlator at large N . We do not present here the explicit expressions for $G_{i_1 \dots i_n}^{(0)}$ and $G_{i_1 \dots i_n}^{(1)}$, they can be found in appendix A of [1].

Combining together the relations (2.13), (2.15) and (2.14), we arrive at the following representation of the partition function (2.8)

$$Z_{\text{QL}} = \mathcal{N} \int D\tilde{J} \exp \left(- \sum_{\alpha=1}^{L-1} \frac{1}{2s_\alpha} C_{ij}^{-1} \tilde{J}_i(p_\alpha) \tilde{J}_j(-p_\alpha) + \sum_{n=1}^{\infty} \frac{1}{N^{n-2} n!} S_n(J) \right), \quad (2.18)$$

where the second term in the exponent is given by a linear combination of homogenous polynomials in J 's with the coefficients defined by the correlators (2.17)

$$S_n(J) = G_{i_1 \dots i_n} \sum_{I=1}^L J_{I,i_1} \dots J_{I,i_n}. \quad (2.19)$$

The exponent of (2.18) has large N expansion analogous to that of the correlator (2.17).

The function $S_n(J)$ has the meaning of an effective action for the sources J_I induced by the double trace interaction (2.6). At large N the leading contribution to the exponent of (2.18) comes from $S_1(J)$. By definition (2.19), it is proportional to the sum of sources at all sites and, therefore, it vanishes $S_1(J) = G_i \sum_{I=1}^L J_{I,i} = 0$ (see (2.16)). We can apply (2.16) to express the remaining $S_n(J)$ with $n \geq 1$ in terms of the sources $\tilde{J}_i(p_\alpha)$

$$S_2 = \sum_{\alpha=1}^{L-1} G_{i_1 i_2} \tilde{J}_{i_1}(p_\alpha) \tilde{J}_{i_2}(-p_\alpha),$$

$$S_n = \frac{1}{L^{n/2-1}} \sum_{\alpha_1, \dots, \alpha_n=1}^{L-1} G_{i_1 \dots i_n} \tilde{J}_{i_1}(p_{\alpha_1}) \dots \tilde{J}_{i_n}(p_{\alpha_n}) \delta(p_{\alpha_1} + \dots + p_{\alpha_n}), \quad (2.20)$$

where the δ -function imposes the condition of conservation of the quasimomentum

$$p_{\alpha_1} + \dots + p_{\alpha_n} = 0 \pmod{2\pi}. \quad (2.21)$$

To simplify formulae we will use a short-hand notation for the sum over quasimomenta in (2.20)

$$S_n \equiv \frac{1}{L^{n/2-1}} G_{i_1 \dots i_n} \tilde{J}_{i_1} \star \dots \star \tilde{J}_{i_n}. \quad (2.22)$$

Finally, we substitute (2.20) into (2.18) to obtain the following representation of the partition function

$$Z_{Q_L} = \mathcal{N} \int D\tilde{J} \exp \left(-\frac{1}{2} \sum_{\alpha=1}^{L-1} \left(\frac{1}{s_\alpha} C_{ij}^{-1} - G_{ij} \right) \tilde{J}_i(p_\alpha) \tilde{J}_j(-p_\alpha) + \sum_{n=3}^{\infty} \frac{G_{i_1 \dots i_n}}{n!(N^2 L)^{n/2-1}} \tilde{J}_{i_1} \star \dots \star \tilde{J}_{i_n} \right). \quad (2.23)$$

This relation depends on two sets of semi-infinite matrices — the expansion coefficients (2.7) and the correlation functions (2.17) in a Gaussian $SU(N)$ matrix model.

The first sum in the exponent of (2.23) is quadratic in the sources $\tilde{J}_i(p_\alpha)$. It describes a propagation of excitations with the quasimomentum p_α along the quiver diagram in figure 1. The second sum in (2.23) describes the interaction between these excitations. The coupling of n excitations is proportional to the correlation functions $G_{i_1 \dots i_n}$ and it is suppressed by the factor of $1/N^{n-2}$. As a consequence, in the leading large N limit the partition function (2.23) is given by a Gaussian integral

$$Z_{Q_L} = \prod_{\alpha=1}^{L-1} \frac{1}{\sqrt{\det(1 - s_\alpha C G)}} + O(1/N^2), \quad (2.24)$$

where the normalization factor \mathcal{N} was replaced with its expression (2.13). Subleading corrections in $1/N$ can be obtained by expanding (2.23) in powers of the interaction term.

Feynman diagram technique. The partition function (2.23) can be evaluated using a Feynman diagram technique. The first term in the exponent of (2.23) defines a propagator of the fields $\tilde{J}_i(p_\alpha)$

$$\langle \tilde{J}_i(p_\alpha) \tilde{J}_j(p_{\alpha'}) \rangle = X_{ij}(p_\alpha) \delta(p_\alpha + p_{\alpha'}), \quad (2.25)$$

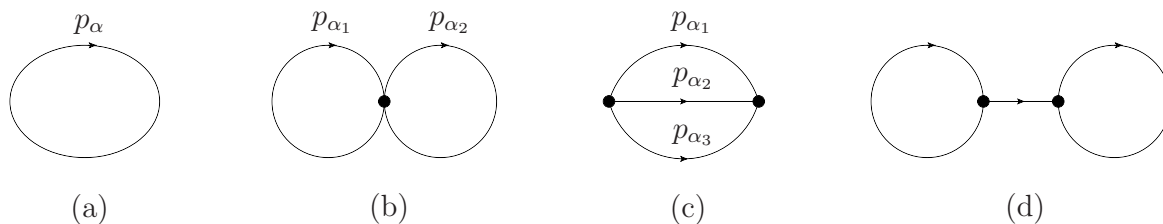


Figure 3. The diagrams contributing to the free energy up to order $O(1/N^2)$. Solid lines represent the propagator (2.25), black dots denote the interaction vertices (2.20). The diagram (d) contains a line with zero momentum exchange and produces a vanishing contribution.

where the δ -function imposes the condition (2.21) and semi-infinite matrix X_{ij} (with $i, j \geq 2$) is defined as

$$X_{ij}(p_\alpha) = \left[s_\alpha C(1 - s_\alpha GC)^{-1} \right]_{ij}. \quad (2.26)$$

We recall that $p_\alpha = 2\pi\alpha/L$ is the quasimomentum of excitations (with $\alpha = 0, \dots, L-1$). Taking into account (2.12) we note that $X_{ij}(p_\alpha)$ vanishes for $\alpha = 0$ and, therefore, the field $\tilde{J}_i(p_\alpha)$ with $p_\alpha = 0$ does not propagate.

The free energy $\Delta F_{Q_L} = -\log Z_{Q_L}$ is given by the sum of ‘vacuum’ Feynman diagrams shown in figure 3. They involve the propagators (2.25) and the interaction vertices generated by the second term in the exponent of (2.23). The contribution of a diagram with h loops scales as $O(1/N^{2(h-1)})$. The diagrams in figure 3 are in the one-to-one correspondence with those shown in figure 2. The former diagrams can be obtained from the latter by simply replacing the chains of touching surfaces by solid lines.

The diagram in figure 3(d) contains an exchange with zero quasimomentum. It produces a vanishing contribution to ΔF_{Q_L} . The contribution of the three remaining diagrams reads

$$\begin{aligned} \Delta F_{Q_L} = & \frac{1}{2} \sum_{\alpha_1=1}^{L-1} \log \det(1 - s_{\alpha_1} CG) \\ & - \frac{1}{8N^2L} \sum_{\alpha_1, \alpha_2=1}^{L-1} G_{i_1 i_2 i_3 i_4} X_{i_1 i_2}(p_{\alpha_1}) X_{i_3 i_4}(p_{\alpha_2}) \\ & - \frac{1}{12N^2L} \sum_{\alpha_1, \alpha_2=1}^{L-1} G_{i_1 i_2 i_3} G_{j_1 j_2 j_3} X_{i_1 j_1}(p_{\alpha_1}) X_{i_2 j_2}(p_{\alpha_2}) X_{i_3 j_3}(-p_{\alpha_1} - p_{\alpha_2}), \end{aligned} \quad (2.27)$$

where summation over repeated indices is tacitly assumed. This relation is valid up to $O(1/N^4)$ corrections. The first term in (2.27) comes from the diagram shown in figure 3(a). Its contribution to ΔF_{Q_L} can be read from (2.24). The second and third terms in (2.27) come from the diagrams shown in figure 3(b) and 3(c), respectively. They are given by the product of the propagators (2.26) and the correlation functions (2.17) summed over the quasimomenta propagating inside the loops.

The relation (2.27) holds for arbitrary L . As explained in the Introduction, ΔF_{Q_L} has to vanish for $L = 1$ to any order in $1/N$. This property holds separately for each term in (2.27). For $L = 2$ the sums in (2.27) contain only one term with $\alpha_1 = \alpha_2 = 1$. In

addition, the last term in (2.27) vanishes because the propagator $X_{i_3 j_3}(-p_{\alpha_1} - p_{\alpha_2})$ carries vanishing quasimomentum $-p_{\alpha_1} - p_{\alpha_2} = 0 \pmod{2\pi}$. The two remaining terms in (2.27) as well as higher order corrections in $1/N$ were computed in [1]. In the next section, we evaluate (2.27) for arbitrary L .

3 Large N expansion of the free energy

The relations (2.26) and (2.27) involve two sets of semi-infinite matrices, C_{ij} and $G_{i_1 \dots i_n}$, defined in (2.7) and (2.17), respectively. The matrix C_{ij} depends on 't Hooft coupling λ and is independent on N . The correlators $G_{i_1 \dots i_n}$ are independent on λ and admit the expansion (2.17) in powers of $1/N^2$.

Replacing the correlators $G_{i_1 \dots i_n}$ in (2.27) with their large N expansion (2.17), we match (2.27) to (1.2) and identify the first two terms of the expansion of the free energy,

$$F_L^{(0)} = \frac{1}{2} \sum_{\alpha=1}^{L-1} \log \det(1 - s_\alpha C G^{(0)}), \tag{3.1}$$

$$F_L^{(1)} = -\frac{1}{2} \sum_{\alpha=1}^{L-1} G_{i_1 i_2}^{(1)} X_{i_1 i_2}^{(0)}(p_\alpha) - \frac{1}{8L} \sum_{\alpha_1, \alpha_2=1}^{L-1} G_{i_1 i_2 i_3 i_4}^{(0)} X_{i_1 i_2}^{(0)}(p_{\alpha_1}) X_{i_3 i_4}^{(0)}(p_{\alpha_2}) - \frac{1}{12L} \sum_{\alpha_1, \alpha_2=1}^{L-1} G_{i_1 i_2 i_3}^{(0)} G_{j_1 j_2 j_3}^{(0)} X_{i_1 j_1}^{(0)}(p_{\alpha_1}) X_{i_2 j_2}^{(0)}(p_{\alpha_2}) X_{i_3 j_3}^{(0)}(-p_{\alpha_1} - p_{\alpha_2}). \tag{3.2}$$

Here $G_{i_1 i_2 \dots}^{(0)}$ and $G_{i_1 i_2 \dots}^{(1)}$ are the first two terms of the large N expansion of the correlator (2.17). The term proportional to $G_{i_1 i_2}^{(1)}$ arises in (3.2) from the expansion of the first term in (2.27) to order $O(1/N^2)$. The propagator $X_{i_1 i_2}^{(0)}(p_\alpha)$ is given by (2.26) with the two-point correlator $G_{i_1 i_2}$ replaced by its leading large N expression $G_{i_1 i_2}^{(0)}$.

3.1 Leading nonplanar correction

We recall that the matrix elements C_{ij} vanish for indices i and j of different parity. Being the two-point correlator in a Gaussian matrix model, the semi-infinite matrix G_{ij} has the same property. In a close analogy with (2.7) we can define nonzero matrix elements $Q_{ij}^+ \equiv G_{2i, 2j}^{(0)}$ and $Q_{ij}^- \equiv G_{2i+1, 2j+1}^{(0)}$ (with $i, j \geq 1$). Then, the relation (3.1) can be simplified as

$$F_L^{(0)} = \frac{1}{2} \sum_{\alpha=1}^{L-1} \left[\log \det(1 - s_\alpha Q^+ C^+) + \log \det(1 - s_\alpha Q^- C^-) \right], \tag{3.3}$$

where the semi-infinite matrices C^\pm were defined in (2.7). Notice that the dependence of $F_L^{(0)}$ on the number of nodes L enters through s_α defined in (2.12).

The properties of semi-infinite matrices $Q^+ C^+$ and $Q^- C^-$ were discussed in [1]. Both matrices are related by a similarity transformation to the same, universal matrix $K_\ell(\chi)$ evaluated for $\ell = 1, 2$

$$\begin{aligned} Q^+ C^+ &= U^+ K_{\ell=1}(\chi) (U^+)^{-1}, \\ Q^- C^- &= U^- K_{\ell=2}(\chi) (U^-)^{-1}. \end{aligned} \tag{3.4}$$

Its matrix elements are given by integral of the product of two Bessel functions of the first kind

$$(K_\ell(\chi))_{ij} = 2(-1)^{i+j} \sqrt{2i+\ell-1} \sqrt{2j+\ell-1} \int_0^\infty \frac{dx}{x} J_{2i+\ell-1}(x) J_{2j+\ell-1}(x) \chi\left(\frac{2\pi x}{\sqrt{\lambda}}\right), \quad (3.5)$$

where $i, j \geq 1$. The function $\chi(x)$ is conventionally called the symbol of the matrix. For the matrices (3.4) it is given by

$$\chi(x) = -\frac{1}{\sinh^2(x/2)}. \quad (3.6)$$

The expression on the right-hand side of (3.3) can be expressed in terms of a determinant of the semi-infinite matrix (3.5)

$$\mathcal{F}_\ell(\chi) = \log \det(1 - K_\ell(\chi)). \quad (3.7)$$

Indeed, the matrices $(1 - s_\alpha \mathbf{Q}^\pm C^\pm)$ entering (3.3) are related by the similarity transformation (3.4) to the matrices $(1 - s_\alpha K_{\ell=1,2}(\chi))$ and, as a consequence, their determinants coincide. Taking into account that $s_\alpha K_\ell(\chi) = K_\ell(s_\alpha \chi)$ we obtain from (3.3)

$$F_L^{(0)} = \frac{1}{2} \sum_{\alpha=1}^{L-1} [\mathcal{F}_{\ell=1}(s_\alpha \chi) + \mathcal{F}_{\ell=2}(s_\alpha \chi)], \quad (3.8)$$

where the function $\mathcal{F}_\ell(s_\alpha \chi)$ is given by (3.7) with the symbol $\chi(x)$ replaced with $s_\alpha \chi(x)$.

For $L = 2$ the relation (3.8) agrees with analogous relation obtained in [1].

3.2 Next-to-leading nonplanar correction

The next-to-leading nonplanar $O(1/N^2)$ correction to the free energy is given by (3.2). Various terms in (3.2) involve the product of semi-infinite matrices defined in (2.26) and (2.17). They can be efficiently computed using the technique developed in [1].

It proves convenient to introduce the so-called Bessel operator

$$\mathbf{K}_\ell = \sum_{i,j \geq 1} |\psi_i\rangle (K_\ell(\chi))_{ij} \langle \psi_j|, \quad (3.9)$$

where $(K_\ell(\chi))_{ij}$ is given by (3.5) and the functions $\psi_i(x)$ (with $i \geq 1$) form an orthonormal basis

$$\begin{aligned} \psi_i(x) &= (-1)^i \sqrt{2i+\ell-1} \frac{J_{2i+\ell-1}(\sqrt{x})}{\sqrt{x}}, \\ \langle \psi_i | \psi_j \rangle &= \int_0^\infty dx \psi_i(x) \psi_j(x) = \delta_{ij}. \end{aligned} \quad (3.10)$$

Then, the product of semi-infinite matrix (3.5) can be evaluated by taking matrix elements of a power of the Bessel operator, e.g. $(K_\ell^n(\chi))_{ij} = \langle \psi_i | \mathbf{K}_\ell^n | \psi_j \rangle$. This property allows us to express (3.7) in terms of a Fredholm determinant of the Bessel operator

$$\mathcal{F}_\ell(\chi) = \log \det(1 - \mathbf{K}_\ell). \quad (3.11)$$

In the similar manner, the infinite sums in (3.2) can be expressed in a concise form in terms of matrix elements of the Bessel operator (3.9).

For $L = 2$ the infinite sums in (3.2) were computed in [1]. In this case they can be expressed in terms of matrix elements of the resolvent of the Bessel operator

$$w_{nm}(\chi) = \langle \phi_n | \chi \frac{1}{1 - \mathbf{K}_\ell} | \phi_m \rangle, \quad (3.12)$$

where the matrix element is evaluated over the states $\phi_n(x)$ (with $n \geq 0$) defined as

$$\phi_0(x) = J_\ell(\sqrt{x}), \quad \phi_n(x) = (x\partial_x)^n \phi_0(x). \quad (3.13)$$

The operator χ in (3.12) has a diagonal kernel and it acts on a test function as $\chi f(x) = \chi(2\pi\sqrt{x/\lambda})f(x)$.

For arbitrary $L \geq 3$, the evaluation of (3.2) goes along the same lines as in [1]. In a close analogy with (3.8), we use (3.12) to define the L -dependent matrix elements

$$w_{nm}(s_\alpha \chi) = s_\alpha \langle \phi_n | \chi \frac{1}{1 - s_\alpha \mathbf{K}_\ell} | \phi_m \rangle, \quad (3.14)$$

where s_α is given by (2.12). Because the operators χ and \mathbf{K}_ℓ are linear in χ , the additional factor of s_α in (3.14) can be absorbed into redefinition of the symbol

$$\chi(x) \rightarrow s_\alpha \chi(x). \quad (3.15)$$

Applying this transformation to (3.12), we arrive at (3.14).

Following [1], we replace the correlation functions $G^{(0)}$ and $G^{(1)}$ in (3.2) with their explicit expressions and express infinite sums in (3.2) in terms of matrix elements (3.14) evaluated for $\ell = 1$ and $\ell = 2$.³ Roughly speaking, each propagator $X_{ij}^{(0)}(p_\alpha)$ in (3.2) gives rise to a linear combination of matrix elements $w_{nm}(s_\alpha \chi)$ with different n and m . Then, the three sums on the right-hand side of (3.2) become homogenous polynomials in matrix elements (3.14) of degree 1, 2 and 3, respectively. Going through the calculation we get

$$\begin{aligned} F_L^{(1)} = & \frac{\langle\langle w_{0,0}^+ \rangle\rangle}{384} + \frac{13\langle\langle w_{0,1}^+ \rangle\rangle}{96} - \frac{\langle\langle w_{0,2}^+ \rangle\rangle}{48} - \frac{\langle\langle w_{1,1}^+ \rangle\rangle}{96} + \frac{13\langle\langle w_{0,0}^- \rangle\rangle}{96} + \frac{5\langle\langle w_{0,1}^- \rangle\rangle}{48} - \frac{\langle\langle w_{0,2}^- \rangle\rangle}{48} - \frac{\langle\langle w_{1,1}^- \rangle\rangle}{96} \\ & - \frac{2}{L} \left[\frac{1}{64} \langle\langle w_{0,0}^+ + w_{0,0}^- \rangle\rangle \langle\langle w_{0,1}^+ + w_{0,1}^- \rangle\rangle + \frac{1}{128} \langle\langle w_{0,0}^+ \rangle\rangle \langle\langle w_{0,0}^- \rangle\rangle + \frac{1}{64} \langle\langle w_{0,0}^- \rangle\rangle^2 + \frac{1}{256} \langle\langle w_{0,0}^+ \rangle\rangle^2 \right] \\ & - \frac{1}{768L} \sum_{\alpha_1, \alpha_2=1}^{L-1} \left(w_{0,0}^+(s_{\alpha_1} \chi) w_{0,0}^+(s_{\alpha_2} \chi) + 3w_{0,0}^-(s_{\alpha_1} \chi) w_{0,0}^-(s_{\alpha_2} \chi) \right) w_{0,0}^+(s_{-\alpha_1 - \alpha_2} \chi), \end{aligned} \quad (3.16)$$

where the notation was introduced for

$$\langle\langle w_{nm}^+ \rangle\rangle = \sum_{\alpha=1}^{L-1} w_{nm}(s_\alpha \chi) \Big|_{\ell=1}, \quad \langle\langle w_{nm}^- \rangle\rangle = \sum_{\alpha=1}^{L-1} w_{nm}(s_\alpha \chi) \Big|_{\ell=2}. \quad (3.17)$$

³We refer the interested reader to [1] for details of the calculation.

The first sum on the right-hand side of (3.2) is given by expression on the first line of (3.16). In a similar manner, the two remaining sums in (3.2) give rise to the second and third lines of (3.16).

For $L = 2$ the relation (3.16) coincides with the analogous expression in the \mathbb{Q}_2 model derived in [1] (see eq. (4.16) there). In this case, the last line of (3.16) vanishes because $s_{-\alpha_1-\alpha_2} = 0$ for $\alpha_1 = \alpha_2 = 1$.

3.3 Nonplanar corrections at weak and strong coupling

The relations (3.8) and (3.16) provide the expressions for the nonplanar corrections to the free energy in terms of the Fredholm determinant of the Bessel operator and the matrix elements of its resolvent, defined in (3.7) and (3.12), respectively. We would like to emphasize that these relations hold for an arbitrary 't Hooft coupling.

Weak coupling. At weak coupling, the calculation of (3.8) and (3.16) simplifies significantly by noticing that the matrix elements (3.5) vanish for $\lambda \rightarrow 0$. To see this, one changes the integration variable in (3.5) as $x \rightarrow \sqrt{\lambda}x$ and replaces the Bessel functions with their small λ expansion to find that $(K_\ell(\chi))_{ij} = O(\lambda^{\ell+i+j-1})$. This property allows us to expand (3.7) in powers of K_ℓ

$$\mathcal{F}_\ell(\chi) = -\text{tr} K_\ell(\chi) - \frac{1}{2} \text{tr} K_\ell^2(\chi) - \frac{1}{3} \text{tr} K_\ell^3(\chi) + O(\lambda^{4(\ell+1)}) \quad (3.18)$$

and, then, replace the semi-infinite matrix (3.5) with its finite-dimensional minor. For the matrix elements (3.12), the analogous expansion is worked out in appendix A (see (A.10)).

Substituting the resulting expressions of $\mathcal{F}_\ell(\chi)$ and $w_{nm}(\chi)$ into (3.8) and (3.16), we find after some algebra

$$\begin{aligned} F_L^{(0)} &= \frac{3\zeta(3)}{64\pi^4} \sigma_2(L) \lambda^2 - \frac{15\zeta(5)}{512\pi^6} \sigma_2(L) \lambda^3 + \left(\frac{315\zeta(7)}{16384\pi^8} \sigma_2(L) - \frac{9\zeta(3)^2}{4096\pi^8} \sigma_4(L) \right) \lambda^4 \\ &+ \left(-\frac{441\zeta(9)}{32768\pi^{10}} \sigma_2(L) + \frac{15\zeta(3)\zeta(5)}{4096\pi^{10}} \sigma_4(L) \right) \lambda^5 + O(\lambda^6), \end{aligned} \quad (3.19)$$

$$\begin{aligned} F_L^{(1)} &= -\frac{3\zeta(3)}{64\pi^4} \sigma_2(L) \lambda^2 + \frac{25\zeta(5)}{512\pi^6} \sigma_2(L) \lambda^3 \\ &+ \left(-\frac{735\zeta(7)}{16384\pi^8} \sigma_2(L) + \frac{9\zeta(3)^2}{2048\pi^8} \left(\sigma_4(L) - \frac{3}{L} \sigma_2^2(L) \right) \right) \lambda^4 + O(\lambda^5), \end{aligned} \quad (3.20)$$

where the dependence on the number of nodes L enters through the functions

$$\sigma_{2n}(L) = \sum_{\alpha=1}^{L-1} s_\alpha^n = \sum_{\alpha=1}^{L-1} \sin^{2n} \left(\frac{\pi\alpha}{L} \right). \quad (3.21)$$

Being combined together, the relations (3.19) and (3.20) yield the weak coupling expansion of the free energy (1.2).

The following comments are in order.

The terms proportional to $\sigma_{2n}(L)$ arise in (3.19) and (3.20) from the expansion of the determinants and matrix elements in powers of $K_\ell(s_\alpha\chi) = s_\alpha K_\ell(\chi)$. The odd Riemann

zeta values come from the integrals $\int_0^\infty dx x^{2n+1} \chi(x) = -4(2n+1)! \zeta(2n+1)$ that arise in the small λ expansion of (3.5).

To high orders in the coupling constant, the leading function $F_L^{(0)}$ is given by multi-linear combinations of odd zeta values multiplied by $\sigma_{2n}(L)$ (see (4.1) below). As compared with the leading large N contribution (3.19), the function $F_L^{(1)}$ contains terms like $\sigma_2^2(L)/L$ that are bilinear in σ . They come from the diagrams shown in figure 3(b) and (c).

Let us examine the dependence of (3.21) on L . For lowest values of n , it is straightforward to check that $\sigma_2(L) = L/2$ for $L \geq 2$, $\sigma_4(L)$ equals 1 for $L = 2$ and $3L/8$ for $L \geq 3$, and so on. The general expression of $\sigma_{2n}(L)$ reads [38]

$$\sigma_{2n}(L) = \begin{cases} 2^{1-2n} L \left[\binom{2n-1}{n-1} + \sum_{p=1}^{\lfloor n/L \rfloor} (-1)^{pL} \binom{2n}{n-pL} \right], & n \geq L, \\ 2^{1-2n} L \binom{2n-1}{n-1}, & n < L. \end{cases} \quad (3.22)$$

Notice that $\sigma_{2n}(L)$ is a linear function of L for $n < L$. This property plays an important role in the next section where we discuss the asymptotic behaviour of the free energy at large L .

For arbitrary n , the function $\sigma_{2n}(L)$ has different L -dependence for $L \leq n$ and $L > n$. The change of the behaviour occurs at $n = L$ and the corresponding function $\sigma_{2L}(L)$ first appears in the weak coupling expansion of the free energy (3.19) at order $O(\lambda^{2L})$. We show in section 4 that this fact has an interesting interpretation in terms of wrapping corrections in the quiver lattice model.

Strong coupling. To derive the strong coupling expansion of the free energy (3.8) and (3.16), we make use of the known properties of the Bessel operator (3.9).

We recall that the leading nonplanar correction to the free energy (3.8) involves the Fredholm determinant of this operator (3.11). The strong coupling expansion of $\mathcal{F}_\ell(\chi)$ for generic symbol $\chi(x)$ was derived in [28, 29]. The first few terms of the expansion are given by

$$\begin{aligned} \mathcal{F}_\ell(\chi) = & -2gI_0(\chi) - \frac{1}{2}(2\ell-1)\log g + B_\ell(\chi) \\ & - \frac{1}{16g}(2\ell-1)(2\ell-3)I_1(\chi) - \frac{1}{64g^2}(2\ell-1)(2\ell-3)I_1^2(\chi) \\ & - \frac{1}{3072g^3}(2\ell-1)(2\ell-3) \left[(2\ell-5)(2\ell+1)I_2(\chi) + 16I_1^3(\chi) \right] + O(1/g^4), \end{aligned} \quad (3.23)$$

where the notation was introduced for

$$g = \frac{\sqrt{\lambda}}{4\pi}. \quad (3.24)$$

The constant term $B_\ell(\chi)$ is conventionally called the Widom-Dyson constant. Its explicit expression can be found in appendix A (see (A.4)). The functions $I_n(\chi)$ (with $n \geq 0$) are defined as

$$I_n(\chi) = \frac{1}{(2n-1)!!} \int_0^\infty \frac{dx}{\pi} (x^{-1} \partial_x)^n x \partial_x \log(1 - \chi(x)). \quad (3.25)$$

High order corrections to (3.23) are given by multi-linear combinations of $I_n(\chi)$.

Substituting (3.23) into (3.8) we encounter the functions $I_n(s_\alpha\chi)$. Replacing $\chi(x)$ and s_α in (3.25) with their expressions, (3.6) and (2.12), respectively, and going through the calculation we find

$$\begin{aligned} I_0(s_\alpha\chi) &= -2\pi \frac{\alpha(L-\alpha)}{L^2}, \\ I_1(s_\alpha\chi) &= -\frac{1}{2\pi} \left[\psi\left(\frac{\alpha}{L}\right) + \psi\left(1 - \frac{\alpha}{L}\right) - 2\psi(1) \right], \end{aligned} \quad (3.26)$$

where $\psi(x) = d \log \Gamma(x)/dx$ is the Euler ψ -function. For arbitrary $n \geq 1$ we have

$$I_n(s_\alpha\chi) = \frac{(-1)^n}{(2\pi)^{2n-1}(2n-2)!} \left[\psi^{(2n-2)}\left(\frac{\alpha}{L}\right) + \psi^{(2n-2)}\left(1 - \frac{\alpha}{L}\right) - 2\psi^{(2n-2)}(1) \right], \quad (3.27)$$

where $\psi^{(n)}(x) = (d/dx)^n \psi(x)$.

To find the nonplanar correction to the free energy (3.16), we use the strong coupling expansion of the matrix elements (3.12) derived in [1]. The matrix element $w_{00}(\chi)$ is given by a derivative of the function (3.7) with respect to the coupling constant

$$w_{00}(\chi) = -4\lambda \partial_\lambda \mathcal{F}_\ell(\chi). \quad (3.28)$$

The remaining matrix elements can be found by taking into account functional relations

$$w_{nm} = w_{mn}, \quad \left(\frac{1}{2} g \partial_g - 1 \right) w_{nm} = \frac{1}{4} w_{0n} w_{0m} + w_{n+1,m} + w_{n,m+1}. \quad (3.29)$$

Note that the relations (3.28) and (3.29) hold for arbitrary 't Hooft coupling λ . The relations (3.29) allow us to express $w_{nm}(\chi)$ for any n and m in terms of independent quantities $w_{0,2n}$ (with $n = 0, 1, \dots$). The strong coupling expansion of w_{00}, w_{01}, w_{11} and w_{02} is given in appendix A, see (A.12).

Substituting the obtained expressions for $\mathcal{F}_\ell(s_\alpha\chi)$ and $w_{nm}(s_\alpha\chi)$ into (3.8) and (3.16), we find after some algebra the following expression for the nonplanar corrections to the free energy

$$F_L^{(0)} = \frac{2(L^2-1)}{3L} g\pi - (L-1) \log g + \frac{1}{2} C_L^{(0)} - \frac{L \log L}{16\pi g} + O(1/g^2), \quad (3.30)$$

$$\begin{aligned} F_L^{(1)} &= -(\pi g)^3 \frac{(L^2-1)(L^2+1)}{30L^3} + (\pi g)^2 \frac{(L^2-1)(L^2-9)}{360L^3} \\ &+ (\pi g) \frac{5(L^2-1)}{384L} + (\pi g) \frac{C_L^{(1)}}{48} + O(g^0), \end{aligned} \quad (3.31)$$

where g is defined in (3.24). The details of the calculation can be found in appendix A.

The coefficient function $C_L^{(0)}$ in (3.30) is given by a linear combination of the Widon-Dyson constant $B_\ell(s_\alpha\chi)$ entering (3.23). Its explicit expression can be found in appendix A, see (A.6). For lowest values of L it looks as

$$\begin{aligned} C_{L=2}^{(0)} &= -12 \log A + 1 - \frac{8}{3} \log 2, \\ C_{L=3}^{(0)} &= -16 \log A + \frac{4}{3} - \frac{17}{6} \log(3) + 2 \log \frac{\Gamma\left(\frac{2}{3}\right)}{\Gamma\left(\frac{1}{3}\right)}, \end{aligned} \quad (3.32)$$

where A is the Glaisher constant. At large L we find that C_L grows linearly with L

$$C_L^{(0)} = L \left(\frac{1}{2} - 12 \log A \right) - 2 \log L + \log(4\pi) + O(1/L). \quad (3.33)$$

The coefficient function $C_L^{(1)}$ in (3.31) is given by

$$C_L^{(1)} = \sum_{\alpha=1}^{L-1} \frac{\alpha}{L} \left(1 - \frac{\alpha}{L} \right) \left[\psi \left(\frac{\alpha}{L} \right) + \psi \left(1 - \frac{\alpha}{L} \right) - 2\psi(1) \right]. \quad (3.34)$$

At large L it behaves as

$$C_L^{(1)} = -L \left(4 \log A - \frac{\gamma}{3} \right) + 1 + O(1/L), \quad (3.35)$$

where γ is the Euler constant.

The relations (3.30) and (3.31) hold for arbitrary number of nodes L . As expected, the functions $F_L^{(0)}$ and $F_L^{(1)}$ vanish for $L = 1$. For $L = 2$ they are in agreement with the expressions derived in [1].

The relations (3.30) and (3.31) were derived at strong coupling and fixed L and, therefore, they are valid for $\sqrt{\lambda} > L$. We observe that at large L all terms in the strong coupling expansion (3.30) and (3.31) except the $O(1/g)$ term in (3.30) scale linearly with L . The asymptotic behaviour of the free energy in the opposite limit, for $L \gg \sqrt{\lambda} \gg 1$ is discussed in the next section.

4 Free energy in the long quiver limit

In this section, we examine asymptotic behaviour of the free energy (1.2) in the limit of large number of nodes L at weak and strong coupling.

Weak coupling. At weak coupling, the dependence of the free energy (1.2) on the number of nodes L can be obtained from (3.19) and (3.20). The expansion coefficients in these relations depend on L through the function $\sigma_{2n}(L)$ given by (3.22).

For instance, the weak coupling expansion of the leading nonplanar correction $F_L^{(0)}$ takes the general form (see (3.19))

$$F_L^{(0)} = \sum_{n \geq 1} \sum_{k_1, \dots, k_n \geq 2} c_{k_1 \dots k_n} \left(\frac{\lambda}{16\pi^2} \right)^{k_1 + \dots + k_n} \sigma_{2n}(L) \zeta_{2k_1-1} \dots \zeta_{2k_n-1}, \quad (4.1)$$

where $c_{k_1 \dots k_n}$ are rational numbers. According to (3.22), the function $\sigma_{2n}(L)$ is linear in L for $n < L$ but this behaviour changes starting from $n = L$.⁴ The function $\sigma_{2n}(L)$ first appears in the expansion (4.1) at $n = L$ and $k_1 = \dots = k_L = 2$. As a result, at weak coupling, the free energy has the asymptotic behaviour (1.3) only up to order $O(\lambda^{2L})$

$$\Delta F_{\mathcal{Q}_L} = L \varepsilon(\lambda, 1/N) + O(\lambda^{2L}). \quad (4.2)$$

⁴The relation (4.1) holds for $L \geq 2$. For $L = 2$ it follows from (3.21) that $\sigma_{2n}(2) = 1$. In the $L \rightarrow \infty$ limit, $\sigma_{2n}(L)$ is replaced with the expression on the second line in (3.22) leading to (1.4).

We apply (3.19) and (3.20) to obtain the energy density at weak coupling as

$$\begin{aligned} \varepsilon(\lambda, 1/N) &= \frac{3\zeta(3)}{128\pi^4} \lambda^2 - \frac{15\zeta(5)}{1024\pi^6} \lambda^3 + O(\lambda^4) \\ &+ \frac{1}{N^2} \left(-\frac{3\zeta(3)}{128\pi^4} \lambda^2 + \frac{25\zeta(5)}{1024\pi^6} \lambda^3 + O(\lambda^4) \right) + O(1/N^4). \end{aligned} \quad (4.3)$$

The breaking of the scaling behaviour (1.3) at order $O(\lambda^{2L})$ is not surprising and has the following interpretation in terms of wrapping, or finite size, effects in the lattice model (2.8).

The partition function (2.8) describes the propagation of excitations across the lattice with L sites. Due to the form of the interaction potential (2.6), excitations at site I can jump to the nearest sites $I \pm 1$. At weak coupling, this produces the $O(\lambda^2)$ contribution to the free energy. The propagation of the excitations across n consecutive sites on the lattice generates correction to the free energy of order $O(\lambda^{2n})$.⁵ For $n < L$ the propagation range is smaller than the circumference of the circle and the corrections to the free energy due to finite size of the system are expected to be small at large L . Starting from $n = L$ the excitations can wrap around the lattice and the finite size effects become important. This explains why the L -dependence of the free energy gets modified at order $O(\lambda^{2L})$.

Strong coupling. At strong coupling, the free energy ΔF_{Q_L} has different dependence on the number of nodes L depending on the ratio $L/\sqrt{\lambda}$.

For $L/\sqrt{\lambda} \ll 1$, it follows from (3.30) that the free energy receives $O(L \log L/\sqrt{\lambda})$ corrections that do not respect the scaling behaviour (1.3). Moreover, examining high order corrections to (3.30), we found that the coefficients of $1/\lambda^{n/2}$ (with $n \geq 2$) are given by polynomials in L of degree n . Retaining the terms with the maximal power of L to each order in $1/\sqrt{\lambda}$, we get

$$F_L^{(0)} = L \left[\frac{1}{6} \sqrt{\lambda} - \log \frac{\sqrt{\lambda}}{4\pi} + \left(\frac{1}{4} - 6 \log A \right) - \frac{\log L}{4\sqrt{\lambda}} \right] - \frac{\sqrt{\lambda}}{6L} + f\left(\frac{L}{\sqrt{\lambda}}\right) + \dots, \quad (4.4)$$

where dots denote terms suppressed by powers of $1/L$. As compared with the strong coupling expansion (3.30), we replaced in (4.4) the coefficients by their leading behaviour at large L and added the subleading corrections in $L/\sqrt{\lambda}$.

These corrections are described by the function $f(l)$ with $l = L/\sqrt{\lambda}$. It is given by⁶

$$\begin{aligned} f(l) &= -\frac{1}{8} l^2 \zeta(2) - \frac{19}{192} l^3 \zeta(3) - \frac{7}{64} l^4 \zeta(4) - \frac{413}{2560} l^5 \zeta(5) - \frac{59}{192} l^6 \zeta(6) \\ &- \frac{83875}{114688} l^7 \zeta(7) - \frac{4315}{2048} l^8 \zeta(8) - \frac{8433167}{1179648} l^9 \zeta(9) - \frac{286081}{10240} l^{10} \zeta(10) + \dots, \end{aligned} \quad (4.5)$$

where dots denote corrections suppressed by $1/g$ as well as exponentially small, nonperturbative corrections. One can show following [39] that the leading nonperturbative correction to (4.5) scales as $O(e^{-2\sqrt{\lambda}/L})$.

The relation (4.5) is well-defined for $l < 1$, or equivalently $1 \ll L < \sqrt{\lambda}$. Substituting (4.5) into (4.4) we find that the free energy does not satisfy (1.3) and has a complicated

⁵See [15] for a diagrammatic interpretation of this property.

⁶To obtain this relation, we used the strong coupling expansion of (3.23) obtained in [29] up to order $O(1/\lambda^{15})$.

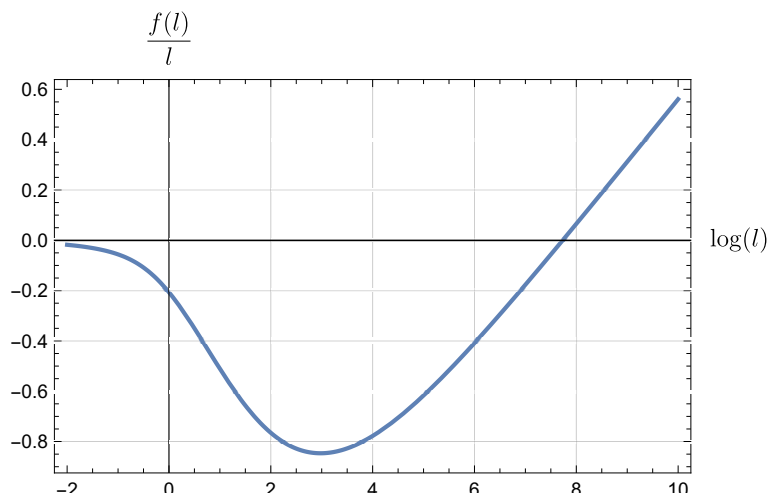


Figure 4. Graphical representation of the function $f(l)/l$ defined in (4.6). At small and large l its behaviour is described by (4.5) and (4.7), respectively.

dependence on the number of nodes L . Namely, $F_L^{(0)}$ contains logarithmically enhanced term $-L \log L/(4\sqrt{\lambda})$ and a nontrivial function $f(L/\sqrt{\lambda})$.

To find the free energy for $1 \ll \sqrt{\lambda} \ll L$ using the strong coupling expansion (4.4), one has to perform a resummation of the series (4.5). This is done in appendix B. As we show there, the function $f(l)$ admits a closed form representation

$$f(l) = \sum_{\alpha=1}^{\infty} \left[\log \left(I_0 \left(\frac{\alpha}{l} \right) I_1 \left(\frac{\alpha}{l} \right) \right) - \frac{2\alpha}{l} + \log \left(\frac{2\pi\alpha}{l} \right) + \frac{l}{4\alpha} \right], \quad (4.6)$$

where $I_0(\alpha/l)$ and $I_1(\alpha/l)$ are the modified Bessel functions (not to be confused with the functions $I_n(\chi)$ defined in (3.25)). The last three terms inside the brackets ensure that the sum converges at large α . It is straightforward to verify that the expansion of (4.6) at small l reproduces the relation (4.5). To see this, it is sufficient to replace the Bessel functions in (4.6) by their asymptotic behaviour at infinity and took into account that $\sum_{\alpha \geq 1} 1/\alpha^n = \zeta(n)$. Notice that the small l expansion of (4.6) also contains exponentially small $O(e^{-2/l})$ corrections.

The dependence of the function (4.6) on $\log l$ is shown in figure 4. We observe that $f(l)/l$ grows linearly with $\log l$. Indeed, for $l \gg 1$ the dominant contribution to the sum in (4.6) comes from $\alpha \ll l$. Keeping the last, leading term inside the brackets in (4.6) we get for $l \gg 1$

$$f(l) \sim \sum_{\alpha=1}^{c'l} \frac{l}{4\alpha} = \frac{l}{4} (\log(4\pi l) - c) + O(l^0), \quad (4.7)$$

where $c = -\gamma - \log(c'/(4\pi)) = 9.714744$.⁷

Substituting (4.7) into (4.4) we observe that troublesome $O(L \log L/\sqrt{\lambda})$ term on the right-hand side of (4.4) cancels against the analogous term coming from (4.7). As a result, the free energy takes the form (1.7) and exhibits the expected scaling behaviour (1.3). The

⁷The constant c was determined by applying the Euler-Maclaurin summation formula to (4.6) at large l .

corresponding expression for the energy density (1.3) looks as

$$\varepsilon(\lambda, 1/N) = \frac{1}{6}\sqrt{\lambda} - \log \frac{\sqrt{\lambda}}{4\pi} + \left(\frac{1}{4} - 6 \log \mathbf{A}\right) - \frac{1}{4\sqrt{\lambda}} \left(\log \frac{\sqrt{\lambda}}{4\pi} + c \right) + O(1/N^2). \quad (4.8)$$

We would like to emphasize that this relation holds for $1 \ll \sqrt{\lambda} \ll L$.

5 Circular Wilson loop

In this section, we compute the expectation value of the circular half-BPS Wilson loop in the \mathbf{Q}_L model. It is defined as

$$W^{\mathbf{Q}_L} = \left\langle \text{tr } P \exp \left(g_{\text{YM}} \oint ds \left[iA_I^\mu(x) \dot{x}_\mu(s) + \frac{1}{\sqrt{2}}(\varphi_I(x) + \varphi_I^*(x)) \right] \right) \right\rangle, \quad (5.1)$$

where the gauge field A_I^μ and complex scalar field $\varphi_I(x)$ are integrated along a circle of unit radius. These fields belong to the $\text{SU}(N)$ $\mathcal{N} = 2$ vector multiplet at node I . The Wilson loop (5.1) does not depend on the choice of the node. In what follows we choose $I = 1$.

For $L = 2$ the Wilson loop (5.1) was computed in the \mathbf{Q}_2 model in [1]. The subsequent analysis of (5.1) goes along the same lines as in that paper. The localization gives the representation of (5.1) as the ratio of expectation values

$$W^{\mathbf{Q}_L} = \frac{\left\langle \text{tr} \left(e^{\sqrt{\frac{\lambda}{2N}} A_1} \right) e^{\sum_I S_{\text{int}}(A_I, A_{I+1})} \right\rangle_0}{\left\langle e^{\sum_I S_{\text{int}}(A_I, A_{I+1})} \right\rangle_0}, \quad (5.2)$$

where the interaction potential $S_{\text{int}}(A_I, A_{I+1})$ is given by (2.6). As before, the subscript ‘0’ indicates that the average is evaluated with the Gaussian measure for the matrices A_I with $I = 1, \dots, L$.

We recall that the interaction potential $S_{\text{int}}(A_I, A_{I+1})$ describes the coupling of the matrices in the adjacent nodes. Neglecting this potential in (5.2) we recover the expectation value of the circular Wilson loop in $\mathcal{N} = 4$ SYM theory

$$W^{\mathcal{N}=4} = \left\langle \text{tr} \left(e^{\sqrt{\frac{\lambda}{2N}} A_1} \right) \right\rangle_0 = \frac{2N}{\sqrt{\lambda}} I_1(\sqrt{\lambda}) + O(1/N). \quad (5.3)$$

The difference between the Wilson loop in the two models $W^{\mathbf{Q}_L} - W^{\mathcal{N}=4}$ arises due to the interaction between the matrices in the different nodes described by (2.6). Due to a peculiar form of the potential (2.6), the interaction does not affect the leading $O(N)$ contribution to (5.2). As a consequence, the Wilson loops $W^{\mathbf{Q}_L}$ and $W^{\mathcal{N}=4}$ coincide in the planar limit. In a close analogy with the free energy (1.1), this suggests to define the difference function

$$\Delta W^{\mathbf{Q}_L} = W^{\mathbf{Q}_L} - W^{\mathcal{N}=4}. \quad (5.4)$$

At large N its expansion starts at order $O(1/N)$.

Expanding (5.2) in powers of A_1 we can express $W^{\mathbf{Q}_L}$ as an infinite sum over expectation value of single traces (2.4)

$$W^{\mathbf{Q}_L} = N + \frac{1}{Z_{\mathbf{Q}_L}} \sum_{n \geq 1} \frac{1}{(2n)!} \left(\frac{\lambda}{2} \right)^n \left\langle \mathcal{O}_{2n}(A_1) e^{\sum_I S_{\text{int}}(A_I, A_{I+1})} \right\rangle_0, \quad (5.5)$$

where $Z_{\mathcal{Q}_L} = \left\langle e^{\sum_I S_{\text{int}}(A_I, A_{I+1})} \right\rangle_0$ is the partition function of the model defined in (2.8). In the absence of the interaction, for $S_{\text{int}}(A_I, A_{I+1}) = 0$, the expectation value $\langle \mathcal{O}_{2n}(A_1) \rangle$ can be obtained by differentiating the generating function (2.15) with respect to the source, $\partial Z(J_1)/\partial J_{1,2n}$. According to (2.13), the interaction term can be generated by averaging this derivative over the source fields with the measure (2.23).

In application to (5.5) this leads to the following representation

$$W^{\mathcal{Q}_L} = N + \sum_{n \geq 1} \frac{1}{(2n)!} \left(\frac{\lambda}{2} \right)^n \left[N G_{2n} + \frac{1}{2N} \langle J_{1,i} J_{1,j} \rangle G_{2n,ij} + O(1/N^3) \right], \quad (5.6)$$

where $G_{2n,ij\dots}$ are connected correlation functions in the Gaussian matrix model (2.17) and $\langle J_{1,i} J_{1,j} \rangle$ denotes an average with respect to the measure (2.23). At large N , we use (2.16) and (2.25) to get

$$\langle J_{1,i} J_{1,j} \rangle = \frac{1}{L} \sum_{\alpha, \alpha'=1}^{L-1} e^{i(p_\alpha + p_{\alpha'})} \langle \tilde{J}_i(p_\alpha) \tilde{J}_j(p_{\alpha'}) \rangle = \frac{1}{L} \sum_{\alpha=1}^{L-1} X_{ij}(p_\alpha), \quad (5.7)$$

where the semi-infinite matrix $X_{ij}(p_\alpha)$ is defined in (2.26). Notice that it is proportional to the interaction matrix C .

In the special case of $\mathcal{N} = 4$ SYM, for $S_{\text{int}}(A_I, A_{I+1}) = 0$, only the first term inside the brackets in (5.6) survives and $W^{\mathcal{N}=4}$ is given by the sum over G_{2n} . Together with (5.4) this leads to

$$\Delta W^{\mathcal{Q}_L} = \frac{1}{2NL} \sum_{n \geq 1} \frac{1}{(2n)!} \left(\frac{\lambda}{2} \right)^n \sum_{\alpha=1}^{L-1} X_{ij}(p_\alpha) G_{2n,ij} + O(1/N^3). \quad (5.8)$$

For $L = 2$ the sum over α contains only one term with the quasimomentum $p = \pi$. In this case, replacing the three-point function $G_{2n,ij}$ with its leading large N expression, one gets [1]

$$\Delta W^{\mathcal{Q}_2} = \frac{1}{16N} \rho \left[w_{00}^+(\chi) + w_{00}^-(\chi) \right] + O(1/N^3), \quad (5.9)$$

where the matrix elements $w_{00}^\pm(\chi)$ are given by (3.17) for $L = 2$ and the notation was introduced for

$$\rho = \sum_{n \geq 1} \frac{1}{(2n)!} \left(\frac{\lambda}{2} \right)^n n(n+1) G_{2n} = \frac{\lambda}{4N} W^{\mathcal{N}=4} + O(1/N^2). \quad (5.10)$$

Here in the second relation we used (5.3).

Going from (5.9) to (5.8), it is sufficient to multiply (5.9) by the factor of $2/L$ and replace the symbol inside the matrix elements $w_{00}^\pm(\chi)$ according to (3.15). This leads to

$$\Delta W^{\mathcal{Q}_L} = \frac{\lambda}{32LN^2} W^{\mathcal{N}=4} \left[\langle\langle w_{00}^+ \rangle\rangle + \langle\langle w_{00}^- \rangle\rangle \right] + O(1/N^3), \quad (5.11)$$

where $\langle\langle w_{00}^\pm \rangle\rangle$ are given by (3.17). Taking into account (3.8) and (3.28) we observe that the sum of matrix elements $\langle\langle w_{00}^+ \rangle\rangle + \langle\langle w_{00}^- \rangle\rangle$ is equal to a derivative of the free energy $(-4g \partial_g F_L^{(0)})$. As a consequence, the relation (5.11) can be written as

$$\Delta W^{\mathcal{Q}_L} = -\frac{\lambda^2}{4LN^2} W^{\mathcal{N}=4} \partial_\lambda F_L^{(0)} + O(1/N^3). \quad (5.12)$$

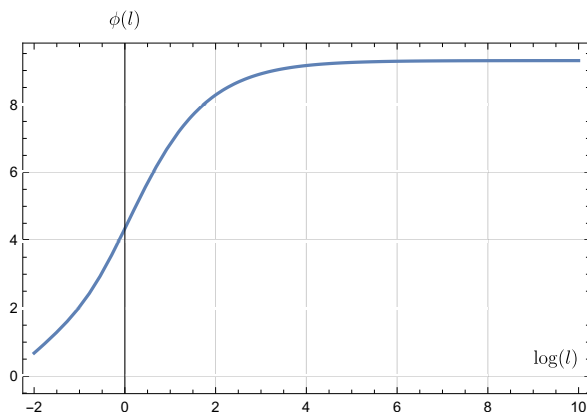


Figure 5. Graphical representation of the function $\phi(l)$ defined in (5.16).

Being combined with (5.4) it leads to the following remarkably simple relation between the ratio of the Wilson loops in the two theories and the free energy

$$\frac{W^{\mathcal{Q}L}}{W^{\mathcal{N}=4}} = 1 - \frac{1}{4LN^2} \lambda^2 \partial_\lambda F_L^{(0)} + O(1/N^4). \quad (5.13)$$

We would like to emphasize that this relation is valid for an arbitrary coupling λ . As expected, the Wilson loops $W^{\mathcal{Q}L}$ and $W^{\mathcal{N}=4}$ coincide in the leading large N limit. It is interesting to note that the nonplanar $O(1/N^2)$ correction to (5.13) is negative for arbitrary coupling.⁸

Let us examine the ratio of Wilson loops (5.13) at large L . At weak coupling we apply (1.3) and (4.3) to find

$$\begin{aligned} \frac{W^{\mathcal{Q}L}}{W^{\mathcal{N}=4}} &= 1 - \frac{1}{4N^2} \lambda^2 \partial_\lambda \varepsilon + O(1/N^4) \\ &= 1 - \frac{1}{N^2} \left[\frac{3\lambda^3 \zeta(3)}{256\pi^4} - \frac{45\lambda^4 \zeta(5)}{4096\pi^6} + O(\lambda^5) \right] + O(1/N^4). \end{aligned} \quad (5.14)$$

Note that the ratio is independent on L and it approaches a finite value for $L \rightarrow \infty$.

At strong coupling, we use (4.4) to obtain from (5.13)

$$\frac{W^{\mathcal{Q}L}}{W^{\mathcal{N}=4}} = 1 - \frac{1}{N^2} \left[\frac{\lambda^{3/2}}{48} - \frac{\lambda}{8} + \frac{1}{32} \sqrt{\lambda} \left(\log \frac{\sqrt{\lambda}}{4\pi} + \phi\left(\frac{L}{\sqrt{\lambda}}\right) \right) \right] + O(1/N^4) + O(1/L), \quad (5.15)$$

where the notation was introduced for

$$\phi(l) = \log(4\pi l) - 4 \frac{df(l)}{dl}. \quad (5.16)$$

The dependence of this function on $\log l$ is shown in figure 5. It grows at small l as $\phi(l) = \log(4\pi l) + \zeta(2)l + O(l^2)$ and for $l \rightarrow \infty$ it approaches a constant $\phi(l) = c - 1$ where c is defined in (4.7).

The relation (5.15) holds for large $\sqrt{\lambda}$ and L . Similar to the free energy, the expression on the right-hand side of (5.15) has different dependence on the number of nodes depending on

⁸Notice that $(-\partial_\lambda \log Z_{\mathcal{Q}L})$ is given by an expectation value of a positive definite function, as follows from (2.1) and (2.2).

how L compares with $\sqrt{\lambda}$. For $L/\sqrt{\lambda} \ll 1$ and $L/\sqrt{\lambda} \gg 1$, the ratio (5.15) is given by (1.10) and (1.9), respectively. Like the energy density (4.8), it ceases to depend on the number of nodes for $1 \ll \sqrt{\lambda} \ll L$. This property requires an explanation.

Acknowledgments

We are very grateful to Arkady Tseytlin for collaboration on subjects closely related to this work. We would like to thank Sergey Frolov, Zohar Komargodski, Paul Krapivsky and Pierfrancesco Urbani for very useful discussions. One of us (G.K.) is grateful to the Hamilton Mathematics Institute at Trinity College Dublin for kind hospitality extended to him where essential part of this work was done.

A Strong coupling expansion

In this appendix, we present some details of derivation of the strong coupling expansion of the free energy (3.30). The expression for $F_L^{(0)}$ can be obtained from (3.8) by replacing the function $\mathcal{F}_\ell(s_\alpha\chi)$ with its asymptotic expression (3.23). This leads to

$$F_L^{(0)} = -2g\langle\langle I_0 \rangle\rangle - \log g + \frac{1}{2}\langle\langle B_{\ell=1} + B_{\ell=2} \rangle\rangle - \frac{1}{16g}\langle\langle I_1 \rangle\rangle - \frac{1}{64g^2}\langle\langle I_1^2 \rangle\rangle + O(1/g^3), \quad (\text{A.1})$$

where the expansion parameter g is defined in (3.24) and $\langle\langle f \rangle\rangle$ denotes the sum of the functions $f(s_\alpha\chi)$ evaluated for possible values of the quasimomentum

$$\langle\langle f \rangle\rangle = \sum_{\alpha=1}^{L-1} f(s_\alpha\chi), \quad s_\alpha = \sin^2\left(\frac{\pi\alpha}{L}\right). \quad (\text{A.2})$$

Taking into account (3.26) and going through the calculation, we get

$$\begin{aligned} \langle\langle I_0 \rangle\rangle &= -\frac{\pi(L^2 - 1)}{3L}, \\ \langle\langle I_1 \rangle\rangle &= \frac{L \log L}{\pi}, \\ \langle\langle I_1^2 \rangle\rangle &= \frac{L(L-1)}{\pi^2} \left[\sum_{\alpha=1}^{L-1} \log^2\left(\sin\left(\frac{\pi\alpha}{L}\right)\right) - L \log^2(2) + \log^2(2L) \right]. \end{aligned} \quad (\text{A.3})$$

Higher order corrections to (A.1) involve sums of the form $\langle\langle I_1^{n_1} I_2^{n_2} \dots \rangle\rangle$ which can be computed in the similar manner.

Widom-Dyson constant. The constant $O(g^0)$ term in (A.1) involves the Widom-Dyson constant $B_\ell(s_\alpha\chi)$. It is given by [28, 29]

$$\begin{aligned} B_\ell(s_\alpha\chi) &= W(\alpha/L) - \frac{1}{2} \log(2\pi) - \frac{\ell}{2} \log(4s_\alpha) + \log \Gamma(\ell), \\ W(\alpha/L) &= \frac{1}{2} \int_0^\infty dk \left[k \left(\tilde{\psi}(k) \right)^2 - \frac{1 - e^{-k}}{k} \right], \\ \tilde{\psi}(k) &= \int_0^\infty \frac{dx}{\pi} \cos(kx) \log(1 - s_\alpha\chi(x)), \end{aligned} \quad (\text{A.4})$$

where $s_\alpha = \sin^2(\pi\alpha/L)$ and $\chi(x) = -1/\sinh^2(x/2)$. Performing integration we find

$$\begin{aligned} \tilde{\psi}(k) &= \frac{2 \sinh(\pi k \frac{\alpha}{L}) \sinh(\pi k(1 - \frac{\alpha}{L}))}{k \sinh(\pi k)}, \\ W(r) &= \frac{1}{2} \log \left[\frac{4\pi^2(2r-1)[G(1-r)G(r)]^4 \cot(\pi r)}{G(1-2r)G(2r-1)} \right], \end{aligned} \tag{A.5}$$

where $r = \alpha/L$ and $G(x)$ is Barnes function. It is easy to check that $W(r) = W(1-r)$. In this way, we obtain the $O(g^0)$ term in (A.1) as

$$C_L \equiv \langle\langle B_{\ell=1} + B_{\ell=2} \rangle\rangle = 2 \sum_{\alpha=1}^{L-1} W(\alpha/L) - (L-1) \log(2\pi) - 3 \log L. \tag{A.6}$$

The explicit expressions for C_L for the few lowest values of L are given by (3.32).

Combining together the above relations we arrive at (3.30).

Matrix elements. The nonplanar correction (3.16) to the free energy $F_L^{(1)}$ depends on the matrix elements of the resolvent of the Bessel operator (3.14).

At weak coupling, we can expand (3.14) in powers of the Bessel operator (3.9) to get

$$w_{nm}(s_\alpha \chi) = s_\alpha \langle \phi_n | \chi | \phi_m \rangle + s_\alpha^2 \langle \phi_n | \chi \mathbf{K}_\ell | \phi_m \rangle + \dots \tag{A.7}$$

The matrix elements on the right-hand side are given by

$$\begin{aligned} \langle \phi_n | \chi | \phi_m \rangle &= \int_0^\infty dx \phi_n(x) \phi_m(x) \chi\left(\frac{\sqrt{x}}{2g}\right) \\ &= (2g)^2 \int_0^\infty dx \phi_n((2g)^2 x) \phi_m((2g)^2 x) \chi(\sqrt{x}) \end{aligned} \tag{A.8}$$

where in the second relation we changed the integration variable $x \rightarrow (2g)^2 x$. Replacing the function $\phi_n(x)$ with its expressions (3.13), one can expand (A.8) in powers of g^2 . In a similar manner, the second term on the right-hand side of (A.7) can be evaluated as

$$\langle \phi_n | \chi \mathbf{K}_\ell | \phi_m \rangle = \sum_{i \geq 1} \langle \phi_n | \chi | \psi_i \rangle \langle \psi_i | \chi | \phi_m \rangle, \tag{A.9}$$

where we took into account that $\mathbf{K}_\ell = \sum_{i \geq 1} |\psi_i\rangle \langle \psi_i| \chi$. Here the matrix elements $\langle \phi_n | \chi | \psi_i \rangle$ are given by (A.8) with ϕ_m replaced by the function ψ_i defined in (3.10). The resulting

expressions for the matrix elements at weak coupling are

$$\begin{aligned}
w_{00}^+(s_\alpha\chi) &= 4g^4q_1 - 4g^6q_2 + g^8\left(2q_1^2 + \frac{5q_3}{3}\right) + \dots, \\
w_{00}^-(s_\alpha\chi) &= g^6q_2 - \frac{2g^8q_3}{3} + \frac{7g^{10}q_4}{36} + \dots, \\
w_{01}^+(s_\alpha\chi) &= 2g^4q_1 - 4g^6q_2 + g^8\left(q_1^2 + \frac{5q_3}{2}\right) + \dots, \\
w_{01}^-(s_\alpha\chi) &= g^6q_2 - g^8q_3 + \frac{7g^{10}q_4}{18} + \dots, \\
w_{11}^+(s_\alpha\chi) &= g^4q_1 - 3g^6q_2 + g^8\left(\frac{q_1^2}{2} + \frac{37q_3}{12}\right) + \dots, \\
w_{11}^-(s_\alpha\chi) &= g^6q_2 - \frac{4g^8q_3}{3} + \frac{25g^{10}q_4}{36} + \dots, \\
w_{02}^+(s_\alpha\chi) &= g^4q_1 - 5g^6q_2 + g^8\left(\frac{q_1^2}{2} + \frac{53q_3}{12}\right) + \dots, \\
w_{02}^-(s_\alpha\chi) &= g^6q_2 - \frac{5g^8q_3}{3} + \frac{31g^{10}q_4}{36} + \dots, \tag{A.10}
\end{aligned}$$

where the superscripts ‘+’ and ‘-’ correspond to $\ell = 1$ and $\ell = 2$, respectively. Here the notation was introduced for

$$q_n = 2s_\alpha \int_0^\infty dx x^{2n+1} \chi(x) = -8s_\alpha(2n+1)!\zeta(2n+1), \tag{A.11}$$

where $\chi(x)$ is given by (3.6). Substituting the relations (A.10) into (3.16) and (3.17), we arrive at (3.20). It is straightforward to verify that the matrix elements (A.10) satisfy the functional relations (3.29).

At strong coupling, we use the expressions for the matrix elements (3.12) derived in [1]

$$\begin{aligned}
w_{00}(\chi) &= 4gI_0 + (2\ell - 1) - \frac{(2\ell - 3)(2\ell - 1)I_1}{8g} - \frac{(2\ell - 3)(2\ell - 1)I_1^2}{16g^2} + \dots \\
w_{01}(\chi) &= -2g^2I_0^2 - 2g\ell I_0 + \frac{1}{8}(2\ell - 1)((2\ell - 3)I_0I_1 - 2\ell - 3) \\
&\quad + \frac{(2\ell - 3)(2\ell - 1)}{16g}I_1(I_0I_1 + \ell + 1) + \dots \\
w_{02}(\chi) &= \frac{2}{3}g^3(I_0^3 - 2I_{-1}) + \frac{1}{2}g^2(2\ell - 1)I_0^2 + g\left(\ell^2I_0 - \frac{1}{16}(2\ell - 3)(2\ell - 1)I_0^2I_1\right) \\
&\quad - \frac{1}{32}(2\ell - 1)\left(I_0^2I_1^2(2\ell - 3) + I_0I_1(2\ell - 3)(2\ell + 1) - 4\ell^2 - 4\ell - 3\right) + \dots \\
w_{11}(\chi) &= \frac{4}{3}g^3(I_0^3 + I_{-1}) + 2g^2\ell I_0^2 + \frac{1}{8}gI_0\left(- (2\ell - 3)(2\ell - 1)I_0I_1 + 4\ell^2 + 8\ell - 3\right) \\
&\quad - \frac{1}{16}(2\ell - 1)\left(I_0^2I_1^2(2\ell - 3) + 2I_0I_1(\ell + 1)(2\ell - 3) - 4\ell - 3\right) + \dots \tag{A.12}
\end{aligned}$$

These relations involve the functions $I_n = I_n(\chi)$. For $n \geq 0$ they are given by (3.25). For $n < 0$ we have instead

$$I_n(\chi) = \int_0^\infty \frac{dx}{\pi} x^{1-2n} \partial_x \log(1 - \chi(x)). \tag{A.13}$$

To obtain the strong coupling expansion of the matrix elements (3.14), it is sufficient to replace $I_n(\chi)$ with $I_n(s_\alpha\chi)$ in (A.12) and apply (3.26) together with

$$I_{-1}(s_\alpha\chi) = -4\pi^3 \frac{(\alpha(L-\alpha))^2}{L^4}. \quad (\text{A.14})$$

The contribution of diagram in figure 3(c). The relations (A.12) allow us to compute expressions on the first two lines of (3.16). The last line of (3.16) describes the contribution of the diagram shown in figure 3(c). It contains a sum over the quasimomenta propagating inside the loops. It is convenient to rewrite this sum as

$$-\frac{1}{768L} \sum_{p_1, p_2, p_3} \delta_{p_1+p_2+p_3} w_{0,0}^+(p_1) \left(w_{0,0}^+(p_2) w_{0,0}^+(p_3) + 3w_{0,0}^-(p_2) w_{0,0}^-(p_3) \right), \quad (\text{A.15})$$

where $w_{0,0}^\pm(p_i) \equiv w_{0,0}^\pm(s_{\alpha_i}\chi)$ and $p_i = 2\pi\alpha_i/L$ (with $1 \leq \alpha_i \leq L-1$).

The δ -function in (A.15) imposes the momentum conservation (2.21). Replacing

$$\delta_{p_1+p_2+p_3} = \frac{1}{L} \sum_{n=1}^L e^{-in(p_1+p_2+p_3)}, \quad \tilde{w}_n^\pm = \sum_{\alpha=1}^{L-1} e^{-inp_\alpha} w_{0,0}^\pm(s_{\alpha_i}\chi) \quad (\text{A.16})$$

we can rewrite (A.15) as

$$-\frac{1}{768L^2} \sum_{n=1}^L \left[(\tilde{w}_n^+)^3 + 3\tilde{w}_n^+ (\tilde{w}_n^-)^2 \right]. \quad (\text{A.17})$$

This sum can be thought of as a discretized version of the integral $\int dx [D(x)]^3$ involving a power of the propagator. By definition, \tilde{w}_n^+ and \tilde{w}_n^- are given by the function

$$\tilde{w}_n = \sum_{\alpha=1}^{L-1} e^{-inp_\alpha} w_{00}(s_\alpha\chi) \quad (\text{A.18})$$

evaluated for $\ell = 1$ and $\ell = 2$, respectively.

Taking into account the first relation in (A.12), we get

$$\tilde{w}_n = \sum_{\alpha=1}^{L-1} e^{-inp_\alpha} \left[4gI_0(s_\alpha\chi) + (2\ell-1) - \frac{(2\ell-3)(2\ell-1)}{8g} I_1(s_\alpha\chi) + O(1/g^2) \right],$$

where $I_0(s_\alpha\chi)$ and $I_1(s_\alpha\chi)$ are given by (3.26). Notice that $\sum_{n=1}^L \tilde{w}_n = 0$. Explicit expression for \tilde{w}_n is different for $1 \leq n \leq L-1$ and $n = L$. In the former case we have

$$\tilde{w}_n = \frac{4\pi g}{L \sin^2(n\pi/L)} - (2\ell-1) - \frac{(2\ell-3)(2\ell-1)}{8g} \sum_{\alpha=1}^{L-1} e^{-inp_\alpha} I_1(s_\alpha\chi) + O(1/g^2). \quad (\text{A.19})$$

For $n = L$ we have instead

$$\tilde{w}_L = -\frac{4\pi g(L-1)(L+1)}{3L} + (2\ell-1)(L-1) - \frac{(2\ell-3)(2\ell-1)}{8g} \frac{L}{\pi} \log L + O(1/g^2). \quad (\text{A.20})$$

These expressions are valid for arbitrary $L \geq 1$.

The functions \tilde{w}_n^+ and \tilde{w}_n^- are given by (A.19) and (A.20) for $\ell = 1$ and $\ell = 2$, respectively. Their substitution into (A.17) leads to

$$(g\pi)^3 \left(\frac{52}{945L^5} - \frac{1}{45L^3} + \frac{11L}{945} - \frac{2}{45L} \right) + (g\pi)^2 \left(-\frac{1}{15L^4} - \frac{1}{18L^3} - \frac{L}{18} + \frac{1}{9L} + \frac{1}{15} \right) + (g\pi) \left(\frac{\langle\langle I_0 I_1 \rangle\rangle}{48L^2} - \frac{\langle\langle I_0^2 I_1 \rangle\rangle}{192\pi} - \frac{\log L}{240L^3} + \frac{1}{6L^2} + \frac{L}{12} - \frac{1}{12L} + \frac{1}{240}L \log(L) - \frac{1}{6} \right) + O(g^0), \tag{A.21}$$

where $\langle\langle I_0^n I_1 \rangle\rangle$ is defined according to (A.2). One can verify that the expression (A.21) vanishes at $L = 2$ as it should be.

The relation (A.21) yields the sum on the last line in (3.16). Adding the contribution of the first two lines in (3.16), we arrive at the relation (3.31). Notice that terms containing $\log L$ and $\langle\langle I_0^2 I_1 \rangle\rangle$ cancel in $F_L^{(1)}$.

B Resummation

In this appendix, we derive the relation (4.6). We recall that the function $f(L/\sqrt{\lambda})$ defines the subleading correction to the free energy (4.4) in the double scaling limit

$$\lambda \gg 1, \quad L \gg 1, \quad L/\sqrt{\lambda} = \text{fixed}. \tag{B.1}$$

Leading behaviour. For arbitrary L the free energy (3.8) is given by the sum over possible values of the quasimomentum $p_\alpha = 2\pi\alpha/L$. At large L , the quasimomentum takes continuous values $0 \leq p \leq 2\pi$. This suggests to rewrite the free energy (3.8) as an integral over p

$$F_L^{(0)} = \frac{L}{2} \sum_{\ell=1,2} \int_0^{2\pi} dp \rho(p) \mathcal{F}_\ell(\sin^2(p/2)\chi). \tag{B.2}$$

Here we replaced s_α with its expression (2.12) and introduced notation for the density function

$$\rho(p) = \frac{1}{L} \sum_{\alpha=0}^{L-1} \delta(p - 2\pi\alpha/L). \tag{B.3}$$

It satisfies the normalization condition $\int_0^{2\pi} dp \rho(p) = 1$ and admits the large L expansion⁹

$$\rho(p) = \frac{1}{2\pi} - \frac{1}{2L}(\delta(p - 2\pi) - \delta(p)) - \frac{\pi}{6L^2}(\delta'(p - 2\pi) - \delta'(p)) + O(1/L^3), \tag{B.4}$$

where prime denote a derivative over p .

At strong coupling, we can replace the function $\mathcal{F}_\ell(\chi)$ in (B.2) by its leading behaviour $\mathcal{F}_\ell(\chi) = -2gI_0(\chi) + O(g^0)$ (see (3.23)). Taking into account (3.25) and (3.6), we obtain the contribution of the first term in (B.4) to (B.2) as

$$-2Lg \int_0^{2\pi} \frac{dp}{2\pi} \int_0^\infty \frac{dx}{\pi} x \partial_x \log \left(1 + \frac{\sin^2(p/2)}{\sinh^2(x/2)} \right) = L \frac{2g\pi}{3}. \tag{B.5}$$

⁹This relation follows from the Euler-Maclaurin summation formula for $\sum_{\alpha=0}^{L-1} \Phi(2\pi\alpha/L) = L \int_0^{2\pi} dp \rho(p) \Phi(p)$ where $\Phi(p)$ is a generic test function.

Repeating the calculation using the $O(1/L)$ term in (B.4), one finds that it yields a vanishing contribution to (B.2). The contribution of the $O(1/L^2)$ term in (B.4) to (B.2) is¹⁰

$$-\frac{g\pi}{6L} \int_0^{2\pi} dp \partial_p \int_0^\infty \frac{dx}{\pi} x \partial_x \log \left(1 + \frac{\sin^2(p/2)}{\sinh^2(x/2)} \right) = -\frac{2g\pi}{3L}. \quad (\text{B.6})$$

Adding together (B.5) and (B.6), we reproduce the first term in the expression (3.30) for $F_L^{(0)}$.

Notice that the integrals (B.5) and (B.6) have different behaviour in the double scaling limit (B.1). Both integrals receive a dominant contribution from $x \sim |\sin(p/2)|$ but the corresponding values of the quasimomentum are different. The leading contribution to (B.5) comes from the region $0 < p < 2\pi$ whereas for (B.6) it only comes from the end-points, $p \rightarrow 0$ and $p \rightarrow 2\pi$, or equivalently $\sin(p/2) \rightarrow 0$.

Subleading corrections to the density function (B.4) give rise to the function f defined in (4.4). An important observation is that, similar to (B.6), it arises from the integration in (B.2) over the end-point region $x \sim |\sin(p/2)|$ and $p \rightarrow 0 \pmod{2\pi}$. In application to (3.23) this implies that, computing the subleading corrections to (B.2), we can replace the symbol $\chi(x)$ in the definition of the function (3.25) with its asymptotic behaviour at small x . According to (3.6), the corresponding symbol is

$$\chi_0(x) = -\frac{4}{x^2}. \quad (\text{B.7})$$

We would like to emphasize that, substituting $\chi(x)$ with $\chi_0(x)$ in (B.2), we only expect to recover the subleading correction to $F_L^{(0)}$ but not the leading one. The latter correction comes from the integration in (B.5) over finite x in which case such substitution is not justified.

Replacing $\chi(x)$ with $\chi_0(x)$ in (B.2) leads to a significant simplification. The main reason is that the function (3.7) can be found in a closed form for the symbol (B.7) (see appendix D in [1])

$$\mathcal{F}_\ell(\chi_0) = \log \left(\Gamma(\ell) \frac{I_{\ell-1}(4g)}{(2g)^{\ell-1}} \right), \quad (\text{B.8})$$

where $I_{\ell-1}(4g)$ is a modified Bessel function of the first kind. To obtain $\mathcal{F}_\ell(s_\alpha \chi_0) = \log \det(1 - K_\ell(s_\alpha \chi_0))$ from (B.8), we take into account that the semi-infinite matrix $K_\ell(s_\alpha \chi_0)$ defined in (3.5) involves the product $s_\alpha \chi_0(x/(2g)) = -4g^2 \sin^2(p_\alpha/2)/x^2$. Because the coupling constant is accompanied by $\sin(p_\alpha/2)$, the dependence of $\mathcal{F}_\ell(s_\alpha \chi_0)$ on s_α can be restored by replacing $g \rightarrow g \sin(p_\alpha/2)$ on the right-hand side of (B.8). In addition, in the end-point region, for $p_\alpha \rightarrow 0$, we can replace $\sin(p_\alpha/2)$ with $p_\alpha/2$. Applying the transformations outlined above, we get from (3.8) and (B.8)

$$F_L^{(0)} \sim \sum_{1 \leq \alpha \ll L} \log \left(\frac{1}{gp_\alpha} I_0(2gp_\alpha) I_1(2gp_\alpha) \right). \quad (\text{B.9})$$

Here we took into account that terms with $\alpha \ll L$ and $(L - \alpha) \ll L$ provide the same contribution to the sum.

¹⁰Here the integral over x gives $2|\sin(p/2)|/\sin(p/2)$ and it approaches opposite values ± 2 for $p \rightarrow 0$ and $p \rightarrow 2\pi$.

By construction, the relation (B.9) captures the contribution to (B.2) from the end-point region $\sin(p/2) \rightarrow 0$. As explained above, we expect that it will generate the function f in the relation (4.4). Indeed, expanding (B.9) at large g we obtain

$$F_L^{(0)} \sim \sum_{1 \leq \alpha \ll L} \left(4gp_\alpha - \log(4\pi g^2 p_\alpha^2) - \frac{1}{8gp_\alpha} - \frac{1}{32g^2 p_\alpha^2} - \frac{19}{1536g^3 p_\alpha^3} - \frac{7}{1024g^4 p_\alpha^4} + \dots \right), \tag{B.10}$$

where $p_\alpha = 2\pi\alpha/L$. We observe that the first three terms inside the brackets provide a contribution that diverges in the double scaling limit (B.1). The contribution of the remaining terms remains finite in this limit. Moreover, replacing $\sum_\alpha 1/p_\alpha^n = L^n \zeta(n)/(2\pi)^n$ as $L \rightarrow \infty$, we find that it correctly reproduces the expansion (4.5) of the function $f(l)$ with $l = L/(4\pi g)$. Subtracting from (B.9) the contribution of the first three terms in (B.10), we arrive at the following relation

$$f = \sum_{\alpha=1}^{\infty} \log \left(4gp_\alpha I_0(2gp_\alpha) I_1(2gp_\alpha) e^{\frac{1}{8gp_\alpha} - 4gp_\alpha} \right). \tag{B.11}$$

It is straightforward to verify that the large g expansion of (B.11) coincides with (4.5) up to exponentially small $O(e^{-8\pi g/L})$ corrections. Replacing $p_\alpha = 2\pi\alpha/L$ and $g = \sqrt{\lambda}/(4\pi)$ in (B.11), we finally arrive at (4.6) with $l = L/\sqrt{\lambda}$.

Open Access. This article is distributed under the terms of the Creative Commons Attribution License ([CC-BY4.0](https://creativecommons.org/licenses/by/4.0/)), which permits any use, distribution and reproduction in any medium, provided the original author(s) and source are credited.

References

- [1] M. Beccaria, G.P. Korchemsky and A.A. Tseytlin, *Non-planar corrections in orbifold/orientifold $\mathcal{N} = 2$ superconformal theories from localization*, *JHEP* **05** (2023) 165 [[arXiv:2303.16305](https://arxiv.org/abs/2303.16305)] [[INSPIRE](https://inspirehep.net/literature/2303163)].
- [2] V. Pestun, *Localization of the four-dimensional $N = 4$ SYM to a two-sphere and 1/8 BPS Wilson loops*, *JHEP* **12** (2012) 067 [[arXiv:0906.0638](https://arxiv.org/abs/0906.0638)] [[INSPIRE](https://inspirehep.net/literature/812873)].
- [3] V. Pestun et al., *Localization techniques in quantum field theories*, *J. Phys. A* **50** (2017) 440301 [[arXiv:1608.02952](https://arxiv.org/abs/1608.02952)] [[INSPIRE](https://inspirehep.net/literature/1608029)].
- [4] A. Pini, D. Rodriguez-Gomez and J.G. Russo, *Large N correlation functions $\mathcal{N} = 2$ superconformal quivers*, *JHEP* **08** (2017) 066 [[arXiv:1701.02315](https://arxiv.org/abs/1701.02315)] [[INSPIRE](https://inspirehep.net/literature/1701023)].
- [5] M. Billò, F. Galvagno and A. Lerda, *BPS wilson loops in generic conformal $\mathcal{N} = 2$ $SU(N)$ SYM theories*, *JHEP* **08** (2019) 108 [[arXiv:1906.07085](https://arxiv.org/abs/1906.07085)] [[INSPIRE](https://inspirehep.net/literature/1906085)].
- [6] B. Fiol, J. Martínez-Montoya and A. Rios Fukelman, *The planar limit of $\mathcal{N} = 2$ superconformal field theories*, *JHEP* **05** (2020) 136 [[arXiv:2003.02879](https://arxiv.org/abs/2003.02879)] [[INSPIRE](https://inspirehep.net/literature/1906085)].
- [7] B. Fiol, J. Martínez-Montoya and A. Rios Fukelman, *The planar limit of $\mathcal{N} = 2$ superconformal quiver theories*, *JHEP* **08** (2020) 161 [[arXiv:2006.06379](https://arxiv.org/abs/2006.06379)] [[INSPIRE](https://inspirehep.net/literature/1906085)].
- [8] S. Kachru and E. Silverstein, *4-D conformal theories and strings on orbifolds*, *Phys. Rev. Lett.* **80** (1998) 4855 [[hep-th/9802183](https://arxiv.org/abs/hep-th/9802183)] [[INSPIRE](https://inspirehep.net/literature/4855)].

- [9] V. Mitev and E. Pomoni, *Exact effective couplings of four dimensional gauge theories with $\mathcal{N} = 2$ supersymmetry*, *Phys. Rev. D* **92** (2015) 125034 [[arXiv:1406.3629](#)] [[INSPIRE](#)].
- [10] V. Mitev and E. Pomoni, *Exact Bremsstrahlung and Effective Couplings*, *JHEP* **06** (2016) 078 [[arXiv:1511.02217](#)] [[INSPIRE](#)].
- [11] B. Fiol, B. Garolera and G. Torrents, *Probing $\mathcal{N} = 2$ superconformal field theories with localization*, *JHEP* **01** (2016) 168 [[arXiv:1511.00616](#)] [[INSPIRE](#)].
- [12] K. Zarembo, *Quiver CFT at strong coupling*, *JHEP* **06** (2020) 055 [[arXiv:2003.00993](#)] [[INSPIRE](#)].
- [13] H. Ouyang, *Wilson loops in circular quiver SCFTs at strong coupling*, *JHEP* **02** (2021) 178 [[arXiv:2011.03531](#)] [[INSPIRE](#)].
- [14] M. Billò et al., *Strong-coupling results for $\mathcal{N} = 2$ superconformal quivers and holography*, *JHEP* **10** (2021) 161 [[arXiv:2109.00559](#)] [[INSPIRE](#)].
- [15] F. Galvagno and M. Preti, *Chiral correlators in $\mathcal{N} = 2$ superconformal quivers*, *JHEP* **05** (2021) 201 [[arXiv:2012.15792](#)] [[INSPIRE](#)].
- [16] M. Beccaria and A.A. Tseytlin, *$1/N$ expansion of circular Wilson loop in $\mathcal{N} = 2$ superconformal $SU(N) \times SU(N)$ quiver*, *JHEP* **04** (2021) 265 [Erratum *ibid.* **01** (2022) 115] [[arXiv:2102.07696](#)] [[INSPIRE](#)].
- [17] M. Billò et al., *Structure Constants in $N = 2$ Superconformal Quiver Theories at Strong Coupling and Holography*, *Phys. Rev. Lett.* **129** (2022) 031602 [[arXiv:2206.13582](#)] [[INSPIRE](#)].
- [18] M. Billò et al., *Localization vs holography in 4d $\mathcal{N} = 2$ quiver theories*, *JHEP* **10** (2022) 020 [[arXiv:2207.08846](#)] [[INSPIRE](#)].
- [19] M. Preti, *Correlators in superconformal quivers made QUICK*, [arXiv:2212.14823](#) [[INSPIRE](#)].
- [20] A.E. Lawrence, N. Nekrasov and C. Vafa, *On conformal field theories in four-dimensions*, *Nucl. Phys. B* **533** (1998) 199 [[hep-th/9803015](#)] [[INSPIRE](#)].
- [21] C.F. Uhlemann, *Exact results for 5d SCFTs of long quiver type*, *JHEP* **11** (2019) 072 [[arXiv:1909.01369](#)] [[INSPIRE](#)].
- [22] C.F. Uhlemann, *AdS_6/CFT_5 with $O7$ -planes*, *JHEP* **04** (2020) 113 [[arXiv:1912.09716](#)] [[INSPIRE](#)].
- [23] L. Coccia, *Topologically twisted index of $T[SU(N)]$ at large N* , *JHEP* **05** (2021) 264 [[arXiv:2006.06578](#)] [[INSPIRE](#)].
- [24] L. Coccia and C.F. Uhlemann, *On the planar limit of 3d $T_\rho^\sigma[SU(N)]$* , *JHEP* **06** (2021) 038 [[arXiv:2011.10050](#)] [[INSPIRE](#)].
- [25] M. Akhond et al., *Matrix models and holography: Mass deformations of long quiver theories in 5d and 3d*, *SciPost Phys.* **15** (2023) 086 [[arXiv:2211.13240](#)] [[INSPIRE](#)].
- [26] C. Nunez, L. Santilli and K. Zarembo, *Linear Quivers at Large- N* , [arXiv:2311.00024](#) [[INSPIRE](#)].
- [27] C.A. Tracy and H. Widom, *Level spacing distributions and the Bessel kernel*, *Commun. Math. Phys.* **161** (1994) 289 [[hep-th/9304063](#)] [[INSPIRE](#)].
- [28] A.V. Belitsky and G.P. Korchemsky, *Octagon at finite coupling*, *JHEP* **07** (2020) 219 [[arXiv:2003.01121](#)] [[INSPIRE](#)].
- [29] A.V. Belitsky and G.P. Korchemsky, *Crossing bridges with strong Szegő limit theorem*, *JHEP* **04** (2021) 257 [[arXiv:2006.01831](#)] [[INSPIRE](#)].

- [30] M. Beccaria, G.V. Dunne and A.A. Tseytlin, *Strong coupling expansion of free energy and BPS Wilson loop in $\mathcal{N} = 2$ superconformal models with fundamental hypermultiplets*, *JHEP* **08** (2021) 102 [[arXiv:2105.14729](#)] [[INSPIRE](#)].
- [31] F. Coronado, *Bootstrapping the Simplest Correlator in Planar $\mathcal{N} = 4$ Supersymmetric Yang-Mills Theory to All Loops*, *Phys. Rev. Lett.* **124** (2020) 171601 [[arXiv:1811.03282](#)] [[INSPIRE](#)].
- [32] A.V. Belitsky and G.P. Korchemsky, *Exact null octagon*, *JHEP* **05** (2020) 070 [[arXiv:1907.13131](#)] [[INSPIRE](#)].
- [33] T. Bargheer, F. Coronado and P. Vieira, *Octagons II: Strong Coupling*, [arXiv:1909.04077](#) [[INSPIRE](#)].
- [34] S.R. Das, A. Dhar, A.M. Sengupta and S.R. Wadia, *New Critical Behavior in $d = 0$ Large N Matrix Models*, *Mod. Phys. Lett. A* **5** (1990) 1041 [[INSPIRE](#)].
- [35] G.P. Korchemsky, *Matrix model perturbed by higher order curvature terms*, *Mod. Phys. Lett. A* **7** (1992) 3081 [[hep-th/9205014](#)] [[INSPIRE](#)].
- [36] L. Alvarez-Gaume, J.L.F. Barbon and C. Crnkovic, *A proposal for strings at $D > 1$* , *Nucl. Phys. B* **394** (1993) 383 [[hep-th/9208026](#)] [[INSPIRE](#)].
- [37] I.R. Klebanov, *Touching random surfaces and Liouville gravity*, *Phys. Rev. D* **51** (1995) 1836 [[hep-th/9407167](#)] [[INSPIRE](#)].
- [38] C.M. da Fonseca, M.L. Glasser and V. Kowalenko, *Basic trigonometric power sums with applications*, [arXiv:1601.07839](#) [[DOI:10.1007/s11139-016-9778-0](#)].
- [39] M. Beccaria, G.P. Korchemsky and A.A. Tseytlin, *Strong coupling expansion in $\mathcal{N} = 2$ superconformal theories and the Bessel kernel*, *JHEP* **09** (2022) 226 [[arXiv:2207.11475](#)] [[INSPIRE](#)].